Deng L, de la Fuente C, Fu P, Wang L, Donnelly R, Wade JD *et al.* (2000). *Virology* **277**: 278–295.
Ginisty H, Sicard H, Roger B, Bouvet P. (1992). *J Cell Sci* **112**: 761–772.
Grinstein E, Wernet P, Snijders PJF, Rosl F, Weinert I, Jia W *et al.* (2002). *J Exp Med* **196**: 1067–1078.
Hamamori Y, Sartorelli V, Ogruzko V, Puri PL, Wu HY, Wang JY *et al.* (1999). *Cell* **96**: 405–413.
Harrod R, Kuo YL, Tang Y, Yao Y, Vassilev A, Nakatani Y *et al.* (2000). *J Biol Chem* **275**: 11852–11857.
Hirano M, Kaneko S, Yamashita T, Luo H, Qin W, Shirota Y *et al.* (2003). *J Biol Chem* **278**: 5109–5115.
Jiang H, Lu H, Schiltz RL, Pise-Masison CA, Ogryzko VV, Nakatani Y *et al.* (1999). *Mol Cell Biol* **19**: 8136–8145.
Kiernan RE, Vanhulle C, Schiltz L, Adam E, Xiao H, Maudoux F *et al.* (1999). *EMBO J* **18**: 6106–6118.
Klibanov S, O'Hagen H, Ljungman M. (2001). *J Cell Sci* **114**: 1867–1873.
Lakin ND, Jackson SP. (1999). *Oncogene* **18**: 7644–7655.
Lang S, Hearing P. (2003). *Oncogene* **22**: 2836–2841.
Lapeyre B, Bourbon H, Amalric F. (1987). *Proc Natl Acad Sci* **84**: 1472–1476.
Lau OD, Coutney AD, Vassilev A, Marzilli LA, Cotter RJ, Nakatani Y *et al.* (2000a). *J Biol Chem* **275**: 21953–21959.
Lau OD, Kundu TK, Soccio RE, Ait-Si-Ali S, Khalil EM, Vassilev A *et al.* (2000b). *Mol Cell* **3**: 589–595.
Levy L, Wei Y, Labalette C, Wu Y, Renard CA, Buendia MA *et al.* (2004). *Mol Cell Biol* **24**: 3404–3414.
Li J, O'Malley BW, Wong J. (2000). *Mol Cell Biol* **20**: 2031–2042.
Luo W, Skalnik DG. (1996). *J Biol Chem* **271**: 23445–23451.
Martinez-Balbas MA, Baner UM, Nielsen SJ, Brehm A, Kouzarides T. (2000). *EMBO J* **19**: 662–671.
Masumi A, Ozato K. (2001). *J Biol Chem* **276**: 20973–20980.
Masumi A, Wang I-M, Lefebvre B, Yang X-J, Nakatani Y, Ozato K. (1999). *Mol Cell Biol* **19**: 1810–1820.
Masumi A, Yamakawa Y, Fukazawa H, Ozato K, Komuro K. (2003). *J Biol Chem* **278**: 25401–25407.
Ott M, Schnolzer M, Gamica J, Fischle W, Emiliani S, Rackwiz HR *et al.* (1999). *Curr Biol* **9**: 1489–1492.
Patel J, Du Y, Ard P, Phillips C, Carella B, Chen C *et al.* (2004). *Mol Cell Biol* **24**: 10826–10834.
Polwsskaya A, Naguibneva I, Duquet A, Bengal E, Robin P, Harel-Bellan A. (2001). *Mol Cell Biol* **21**: 5312–5320.
Santos-Rosa H, Valls1 E, Kouzarides T, Martinez-Balbas M. (2003). *Nucl Acids Res* **31**: 4285–4292.
Schaffer BC, Paulson E, Strominger JL, Speck SH. (1997). *Mol Cell Biol* **17**: 873–886.
Schiltz RL, Mizzen CA, Vassilev A, Cook RG, Allis CD, Nakatani Y. (1999). *J Biol Chem* **274**: 1189–1192.
Spilianakis C, Papamatheakis J, Kretsovail A. (2000). *Mol Cell Biol* **20**: 8489–8498.
Srivastava M, Pollard HB. (1999). *FASEB J* **13**: 1911–1922.
Stellacci E, Testa U, Retrucci E, Benedetti E, Orsatti R, Feccia T *et al.* (2004). *Biochem J* **377**: 367–378.
Sterner DE, Berger SL. (2000). *Mol Cell Biol* **64**: 435–459.
Suhara W, Yoneyama M, Kitabayashi I, Fujita T. (2002). *J Biol Chem* **277**: 22304–22313.
Taniguchi T, Ogasawara K, Takaoka A, Tanaka N. (2001). *Annu Rev Immunol* **19**: 623–655.
Trievel RC, Li FY, Mamorstein R. (2000). *Anal Biochem* **287**: 319–328.
Vassilev A, Yamauchi J, Kotani T, Prives C, Avantaggiati ML, Qin J *et al.* (1998). *Mol Cell* **2**: 869–875.
Vaughan PS, van der Meijden CM, Aziz F, Harada H, Taniguchi T, van WA *et al.* (1998). *J Biol Chem* **273**: 194–199.
Vo N, Goodman RH. (2001). *J Biol Chem* **276**: 13505–13508.
Wang I-M, Blanco JCG, Tsai SY, Tsai M-J, Ozato K. (1996). *Mol Cell Biol* **16**: 6313–6324.
Wolf D, Rodova M, Miska EA, Calvet JP, Kouzarides T. (2002). *J Biol Chem* **28**: 25562–25567.
Xie R, van Wijnen AJ, van der Meijden C, Luong MX, Stein JL, Stein GS. (2001). *J BIol Chem* **276**: 18624–18632.
Yamamoto H, Lamphier M, Fujita T, Taniguchi T, Harada H. (1994). *Oncogene* **9**: 1423–1428.
Yamauchi T, Yamauchi J, Kuwata T, Tamura T, Yamashita T, Bae N *et al.* (2000). *Proc Natl Acad Sci USA* **97**: 11303–11306.
Yanagida M, Shimamoto A, Nishikawa K, Furuichi Y, Takahashi N. (2001). *Proteomics* **1**: 1390–1404.
Ying G-G, Proost P, van Damme J, Bruschi M, Introna M, Golay J. (2000). *J Biol Chem* **275**: 4152–4158.
Yoneyama M, Suhara W, Fukuhara Y, Fukuda M, Nishida E, Fujita T. (1998). *EMBO J* **17**: 1087–1095.

ELSEVIER

INSTITUT PASTEUR

Microbes and Infection 9 (2007) 515–521

www.elsevier.com/locate/micinf

Original article

GBV-B as a pleiotropic virus: distribution of GBV-B in extrahepatic tissues *in vivo*

Koji Ishii [a], Sayuki Iijima [b], Nobuyuki Kimura [b], Young-Jung Lee [b], Naohide Ageyama [b], Shintaro Yagi [d,1], Kenjiro Yamaguchi [d], Noboru Maki [d], Ken-ichi Mori [d], Sayaka Yoshizaki [a], Sanae Machida [a,e], Tetsuro Suzuki [a], Naoko Iwata [c], Tetsutaro Sata [c], Keiji Terao [b], Tatsuo Miyamura [a], Hirofumi Akari [b,*]

[a] *Department of Virology II, National Institute of Infectious Diseases, 1-23-1 Toyama, Shinjuku-ku, Tokyo 162-8640, Japan*
[b] *Laboratory of Disease Control, Tsukuba Primate Research Center, National Institute of Biomedical Innovation, 1-1 Hachimandai, Tsukuba, Ibaraki 305-0843, Japan*
[c] *Department of Pathology, National Institute of Infectious Diseases, 1-23-1 Toyama, Shinjuku-ku, Tokyo 162-8640, Japan*
[d] *Advanced Life Science Institute, Wako, Saitama 351-0112, Japan*
[e] *Department of Microbiology, Saitama Medical School, Moroyama-Cho, Iruma-Gun, Saitama 350-0495, Japan*

Received 25 August 2006; accepted 16 January 2007
Available online 27 January 2007

Abstract

GB virus B (GBV-B) infection of New World monkeys is considered to be a useful surrogate model for hepatitis C virus (HCV) infection. GBV-B replicates in the liver and induces acute resolving hepatitis but little is known whether the other organs could be permissive for the virus. We investigated the viral tropism of GBV-B in tamarins in the acute stage of viral infection and found that the viral genomic RNA could be detected in a variety of tissues. Notably, a GBV-B-infected tamarin with marked acute viremia scarcely showed a sign of hepatitis, due to preferential infection in lymphoid tissues such as lymph nodes and spleen. These results indicate that GBV-B as well as HCV is a pleiotropic virus *in vivo*.

Keywords: GB virus B; Hepatitis C virus; Tamarin; Surrogate model

1. Introduction

Over 100 million people worldwide are carriers of hepatitis C virus (HCV) and the viral infection is a significant cause of human morbidity and mortality; chronic HCV infection in many cases will lead to liver cirrhosis and hepatocellular carcinoma. Furthermore, HCV infection manifests a variety of extrahepatic, at least in part due to the extrahepatic tropisms of HCV, particularly lymphotropism diseases (for review see [1]).

Other than humans, only chimpanzees that are endangered as species can be productively infected by HCV. Together with ethical issues regarding animal experiments, it has becomes increasingly difficult to access chimpanzees for experimental studies. Tamarins (*Saguinus* species), one of the new world monkeys, develop acute, self-limited hepatitis upon infection with the GB virus B (GBV-B), which is most closely related to HCV [2–4]. Although the acute nature of GBV-B infection in tamarins has been distinguished this hepatitis from HCV infection in humans, recent studies demonstrated that tamarins could be persistently infected by GBV-B and developed chronic hepatitis [5,6]. Therefore, the GBV-B infection of tamarins is proposed as a good surrogate model for hepatitis C. While GBV-B appeared to infect liver, comprehensive documentation of the *in vivo* tropism of GBV-B has not been

* Corresponding author. Tel.: +81 29 837 2121; fax: +81 29 837 0218.
E-mail address: akari@nibio.go.jp (H. Akari).
[1] Present address: Laboratory of Cellular Biochemistry, Department of Animal Resource Sciences, Graduate School of Agricultural and Life Sciences, The University of Tokyo, Tokyo, Japan.

1286-4579/$ - see front matter © 2007 Elsevier Masson SAS. All rights reserved.
doi:10.1016/j.micinf.2007.01.010

reported yet. A previous report that GBV-B RNA was observed in peripheral blood mononuclear cells (PBMCs) from a GBV-B-infected marmoset [7] suggests that GBV-B may be lymphotropic as well as HCV. Considering the close similarity between HCV and GBV-B, we examined the viral distribution and tropism in tamarins in the acute phase of the viral infection.

2. Materials and methods

2.1. Animals

Adult white-lipped and Red-handed tamarins (*Saguinus labiatus* and *Saguinus midas*, respectively) were housed in individual cages at the Tsukuba Primate Research Center. All animal studies were conducted in accordance with the protocols of experimental procedures that were approved by the Animal Welfare and Animal Care Committees of the National Institute of Biomedical Innovation and National Institute of Infectious Diseases. The details of tamarins used in this study were summarized in Table 1.

2.2. GBV-B infection in tamarins

GBV-B RNA was transcribed *in vitro* with T7 RNA polymerase (Promega, Madison, WI) from 10 μg of *Xho*I-digested pGBB [2] that harbors infectious cDNA for GBV-B (kind gift of Dr. J. Bukh, National Institutes of Health, USA). The integrity of the RNA was checked by electrophoresis through an agarose gel stained with ethidium bromide. Each transcription mixture (400 μg of GBV-B RNA) was diluted with 400 μl of ice-cold water and then immediately frozen on dry ice and stored at −80 °C. Transcription mixtures were injected into each tamarin intrahepatically. For transmission of GBV-B, animals were infected intrahepatically with 100 μl of GBV-B infectious plasma containing 8×10^8 genome equivalents (GE) of the viral RNA. Blood samples were periodically collected from the monkeys from femoral vein under anesthetization and were tested for plasma ALT level.

2.3. Quantification of GBV-B genomic RNA

GBV-B-infected tamarins were euthanized and perfused with saline thoroughly before the collection of specimens including plasma, PBMCs and a variety of tissues (esophagus, stomach, duodenum, jejunum, ileum, cecum, colon, rectum, liver, pancreas, submandibular gland, trachea, lung, bone marrow, thymus, spleen, submandibular lymph nodes, axillary lymph nodes, intestinal lymph nodes, mesenteric lymph nodes, inguinal lymph nodes, tonsil, heart, kidney, adrenal gland, bladder, brain, spinal cord, testis, uterus and ovary). GBV-B RNA from these specimens was quantified by a real-time, 5′ exonuclease PCR (TaqMan) assay using a primer-probe combination that recognized a portion of the GBV-B capsid gene. The primers 558F [5′AACGAGCAAAGCGCAAAGTC] and 626R [5′CATCATGGATACCAGCAATTTTGT] and probe 579P [5′6FAM-AGCGCGATGCTCGGCCTCGTATAMRA] [8] were obtained from PE Biosystems. The primers were used at 15 pmol/50 μl reaction, and the probe was used at 10 pmol/50 μl reaction. Synthesized GBV-B RNA was used as a reference standard of GBV-positive plasma. PBMCs were isolated from whole blood by density-gradient centrifugation. Approximately 10 mg of tissues were removed under sterile conditions and immediately homogenized in 1 ml of TRIzol (Invitrogen, Carlsbad, CA) to extract RNA. We set our lowest detection cutoff at 10^2 GE per ml. All the specimens were evaluated in duplicates and the averages were shown.

Table 1
Summary of the results of GBV-B RNA levels in the tissues of the virus-infected tamarins

		Tm3	Tm4	Tm5	Tm6
Animals		*S. labiatus*	*S. midas*	*S. labiatus*	*S. midas*
Sex		Female	Female	Male	Female
GBV-B inoculum		Plasma	Plasma	RNA	RNA
Weeks at necropsy		4	4	3	ND[a]
ALT		321	522	38	554
Viral loads in:					
Blood	Plasma	3.8×10^8	5.9×10^8	1.3×10^{10}	2.8×10^9
	PBMC	270	1630	35650	ND
Spleen		(−)[b]	540	5980	ND
Lymph nodes	Inguinal	(−)	(−)	3090	ND
	Intestinal	(−)	(−)	640	ND
Liver		70080	33480	16080	ND
Kidney		(−)	(−)	380	ND
Testis				600	ND
Ovary		1290	150		ND
Bone marrow		120	(−)	750	ND

Viral loads in each tissues were presented as GE/mg except for plasma (GE/ml) and PBMC (GE/10^6 cells). Data for Tm6 were obtained at week 4.
[a] ND: not done.
[b] (−): undetectable.

2.4. Detection of anti-GBV-B core and NS3 antibodies by ELISA

The TrpE-core (aa 1 to 132) fusion protein and TrpE-NS3 (aa 1135 to 1378) fusion protein, representing a portion of NS3 identified as being immunogenic in infected animals [9], was expressed in *Escherichia coli* [10] to serve as an antigen to generate polyclonal rabbit antisera. Tamarin sera were tested for the presence of antibodies to GBV-B core and NS3 by ELISA as described previously [8].

2.5. Cloning of entire GBV-B genome from plasma, liver and PBMCs of infected tamarins

GBV-B RNA was isolated from plasma, liver and PBMCs as described above. GBV-B cDNA was synthesized using Super-Script reverse transcriptase II (Invitrogen) with GB-5145R primer (5′-GCG AGT GCG GCT GTC CCA GAA GTA TTG ACT-3′) or GB-9051R primer (5′-AAT TTG GGG GTT CAG CTG ATG GCT AAT CCA-3′). After RNase H (Invitrogen) treatment at 42 °C, a cDNA mixture was subjected to PCR with LA-taq DNA polymerase (TaKaRa), GB-5145R primer and GB-35S primer (5′-ACC ACA AAC ACT CCA GTT TGT TAC ACT CCG CTA GG-3′) or GB-9051R primer and GB-3999S primer (5′-CGT ACG GCG TGA ATC CAA ATT GCT ATT TTA-3′) for 30 cycles of denaturation at 94 °C for 20 s and extension at 68 °C for 5 min. PCR products were purified from the gel using a QIA-quick gel kit (Qiagen), and then cloned into pGEM-T Easy vector (Promega). Four clones of each fragment were determined using a CEQ-2000XL analysis system with a DTCS quick start kit and GBV-B specific primers according to the manufacturer's instructions. Sequence data were analyzed on Macintosh computers with the Sequencer (Gene Code Corp.) and MacVector (Accelrys) software packages.

2.6. Synthesis of positive and negative standard RNAs for RT–PCR controls

Recombinant positive and negative strand RNAs were generated from pGBB containing 3′ sequences of GBV-B. Positions 8569–9359 were amplified and inserted into pGEM-T easy vector. Clones were selected for sense and antisense orientation of the insert corresponding to positive and negative strands, respectively. Ten micrograms of the selected plasmids were linearized using *Pst*I and positive- and negative-strand RNAs were synthesized by transcription from the upstream T7 RNA polymerase promoter by Ambion MEGAscript T7 kit (Ambion, Austin, TX).

2.7. Detection of strand-specific viral RNA by tagging PCR system

One microgram of total RNA obtained from tissues or cells was subjected to RT–PCR. cDNAs were synthesized using Superscript III first strand synthesis system (Invitrogen). In order to overcome the detection of falsely primed cDNA products and make the PCR system strand-specific, additional nucleotides (TCATGGTGGCGAATAA) were added to the 5′ end of the reverse transcription primer (5′-TCATGGTGGC GAATAATTGGATTAGCCATCAGCTGAACC-3′), forming a "tag" (underlined) [11,12]. This "tag" sequence was neither complementary nor homologous to any part of the GBV-B genome. PCR amplification of a tagged cDNA was performed using only the tag portion of the cDNA primer (5′-TCATGG TGGCGAATAA-3′) as one of the primers and a GBV-B specific oligonucleotide for the opposing primer (5′-CTTGGTAC TACGCTCTGCACA-3′, positions 9339–9359). For the first round of PCR using 2 µl of cDNA in a final volume of 25 µl, the reactions were performed using a TaKaRa PCR kit (TaKaRa) with following conditions; a 20 s and 94 °C denaturation step followed by 20 s and 55 °C annealing and 2 min and 72 °C extension steps. After 30 cycles of first round amplification, 2 µl of reaction samples were subjected to 30 cycles of nested PCR using 5′-TTTTAGGGCAGCGGCAACAG-3′ (positions 9105–9124) and 5′-CACACAGCCAGGACTCCTCA-3′ (positions 9260–9279) as primers.

2.8. Histopathology

Five tamarin livers were used in this study. Of these, three livers were from GBV-B-infected tamarins (Table 1), and two were from uninfected tamarins. Liver samples obtained by necropsy were fixed with 4% paraformaldehyde, embedded in paraffin, and cut into 4 µm thick-sections. Deparaffinized sections were stained with hematoxylin and eosin (H&E) for histopathological analyses. To investigate apoptotic cells in the livers, we also examined both DNA fragmentation and immunohistochemistry for an active form of caspase-3. To diminish autofluorescence mainly caused by lipofuscin, sections were pre-stained with 1% Sudan black B. DNA fragmentation was evaluated by a TUNEL assay with an ApopTag Direct *In Situ* Apoptosis Detection Kit (Chemicon International, Temecula, CA) according to the manufacturer's instructions. Briefly, the specimens were digested with a solution of proteinase K (20 µg/ml) in PBS for 5 min and then incubated with terminal deoxynucleotidyl transferase (TdT) and fluorescein-labeled nucleotides (ApopTag Direct) in a humid atmosphere at 37 °C for 1 h. Specimens were viewed with a BX-FLA fluorescence microscope (Olympus, Tokyo, Japan). To control for nonspecific incorporation of nucleotides and nonspecific binding of TdT, cells were treated with proteinase K as usual, but staining was performed in the absence of active TdT. This served as a negative control. In parallel, immunohistochemistry for an active form of caspase-3 was examined by using an FITC-conjugated monoclonal antibody against the active caspase-3 (C92-605; BD Pharmingen, San Jose, CA) in order to confirm the degree of apoptotic cells detected by TUNEL staining. Sections were deparaffinized followed by autoclaving for 5 min at 121 °C, and then incubated free floating in the primary antibody solution overnight at 4 °C. Following brief washes, sections were then incubated with DAPI (1:800; Santa Cruz Biotechnology, Santa Cruz, CA) for 1 h at room temperature. These sections were examined with a Digital Eclipse C1 confocal microscope (Nikon, Japan).

3. Results

3.1. GBV-B infection in tamarins

Firstly, two tamarins were intrahepatically inoculated with RNA transcripts from GBV-B infectious molecular clone pGBB (Fig. 1). Both monkeys showed viremia at 2 weeks post inoculation; peak viral titers in plasma reached up to 10^9 GE/ml and both monkeys developed hepatitis with dramatically elevated plasma ALT levels. The viremia was maintained up to 8 weeks, followed by rapid decline in parallel with the resolution of the ALT abnormalities. Within 6–8 weeks of the inoculation, the development of antibodies reactive with the viral core and NS3 proteins was observed (Fig. 1). Multiple plasma samples collected at later time points contained no detectable viral RNA and showed no ALT abnormalities; however, antibodies against GBV-B core and NS3 proteins were maintained at relatively high levels at least until 28 weeks after inoculation (Fig. 1). These results confirmed that inoculation of GBV-B viral RNA caused acute hepatitis in parallel with typical viremia in tamarins.

Next, in order to examine the tissue tropism of GBV-B *in vivo*, four tamarins were inoculated intrahepatically with week 2 plasma of tamarin Tm1 containing 8×10^8 GE of GBV-B (Tm3 and Tm4) or synthetic GBV-B RNA as described above (Tm5 and Tm6). These tamarins developed a typical acute infection that were marked by high levels of viremia, indicating that inoculation of either viral RNA or plasma of the infected tamarin resulted in comparable outcome (Fig. 2). It is noteworthy that in Tm5 the plasma ALT level was scarcely elevated in contrast with other three tamarins during the acute period of GBV-B infection, although this tamarin developed highest viremia (1.3×10^{10} GE/ml).

3.2. Histopathological analyses of GBV-B infection

Histopathological analyses in Tm3 and Tm4 livers showed inflammatory responses including inflammatory cell invasions around central and/or portal veins and hemorrhages, hepatocytic degenerations, and disruptions of sinusoids (Fig. 3A,B,E,F). Although there were only minimal pathological changes, hepatocytic degenerations and dilation of sinusoids were also found in the Tm5 liver (Fig. 3C and G) in contrast to uninfected tamarins (Fig. 3D and H, data not shown). To further evaluate the levels of apoptotic hepatocytes in these monkeys, we employed two different methods, detecting fragmented DNA (TUNEL assay) and an active form of caspase-3 as previously described [13]. It was found that substantial numbers of fragmented DNA-positive cells were observed in the Tm3 and Tm4 livers while much less in the Tm5 liver (Fig. 3I–K). Consistent results were obtained when the active form of caspase-3 was stained (Fig. 3M–O). On the other hand, we found neither DNA fragmentation nor caspase-3 activation in uninfected tamarin livers (Fig. 3L and P, data not shown). The minimal levels of pathological changes in the Tm5 liver were well correlated with a lower level of plasma ALT in Tm5 (Fig. 2, Table 1).

3.3. Tissue distribution of GBV-B

The results described above suggested the possibility that the substantial levels of viral replication occurred in other tissues rather than in the liver of Tm5. To ascertain the possibility, we euthanized three tamarins (Tm3, Tm4 and Tm5) and the viral levels in a variety of tissues were compared. Table 1 summarizes the data obtained in this experiment. It is reasonable to consider that GBV-B replicated in the liver accounts for majority of the viral load *in vivo*. However,

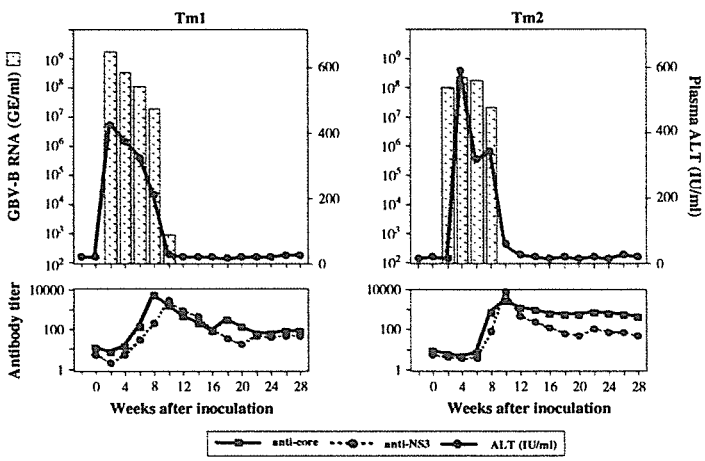

Fig. 1. Course of GBV-B infection in tamarins Tm1 and Tm2. Synthesized infectious RNA transcript of GBV-B from a pGBB molecular clone was inoculated into each tamarin intrahepatically. Plasma samples were collected from each tamarin at 2-week intervals post inoculation. The viral RNA copies, ALT levels, and titers of anti-viral antibodies (anti-core and anti-NS3) in the plasma samples until 28 weeks after inoculation were shown.

substantial levels of GBV-B RNA were detected not only in the liver but also in a variety of extrahepatic tissues such as hematolymphoid and genital tissues, suggesting that GBV-B may infect and replicate in these organs. Notably, the viral RNA levels of Tm5 were much greater in the lymphoid tissues but lower in the liver as compared with those of other two tamarins, indicating that the highest plasma viral load in Tm5 derived from extrahepatic tissues, mainly hematolymphoid tissues. We could not detect GBV-B RNA from other tissues tested (data not shown). From these results, we concluded that the preferential distribution of GBV-B in the extrahepatic tissues rather than in the liver of Tm5 may attribute to the highest plasma viral load in spite of the mild disorder and the lower viral load in the liver.

In addition, the unique viral distribution implied that the GBV-B disseminated in Tm5 might acquire novel tissue tropism as a result of genomic mutation. To ascertain the possibility, we amplified the entire viral genomes by RT–PCR from the liver, PBMCs and plasma collected from Tm5 at euthanasia and compared with the original nucleotide sequence. The sequences determined were completely identical to the original sequence of GBV-B (data not shown), indicating that the sequence heterogeneity of GBV-B was not responsible for the different tropism observed in Tm5 and thus GBV-B intrinsically exhibits pleiotropism in a host-dependent manner.

3.4. Detection of strand-specific viral RNA in the tamarin tissues

To confirm that the virus was actually replicated in the tissues other than the liver, we sought to deferentially determine negative-strand viral RNA which is shown to be a viral replication intermediate in case of HCV. We thus newly developed an assay system for detecting replication intermediate of GBV-B.

To determine the sensitivity of this method, synthetic positive- and negative-strand GBV-B transcripts (ranging from 10^8 to 10^0 copies of GBV-B) in 100-fold serial dilutions were subjected to RT–PCR. As shown in Fig. 4A, at least 100 copies of GBV-B negative-strand RNA could be detected by this method. When the primer for cDNA synthesis was omitted, no PCR products were obtained (Fig. 4A, negative control), indicating that the PCR signals were derived specifically from the GBV-B negative-strand RNA. In the presence of 10^8 copies of positive-strand HCV RNA, false positive PCR signals appeared (Fig. 4A). We then analyzed the samples from liver, spleen, pancreas, stomach and PBMCs from Tm5 using the GBV-B strand-specific PCR assay and found that the negative-strand viral RNAs were detected in the liver, spleen and PBMC samples (Fig. 4B). No negative-strand or replicating forms of the virus were detected from RNA extracted from pancreas, stomach and HeLa cells.

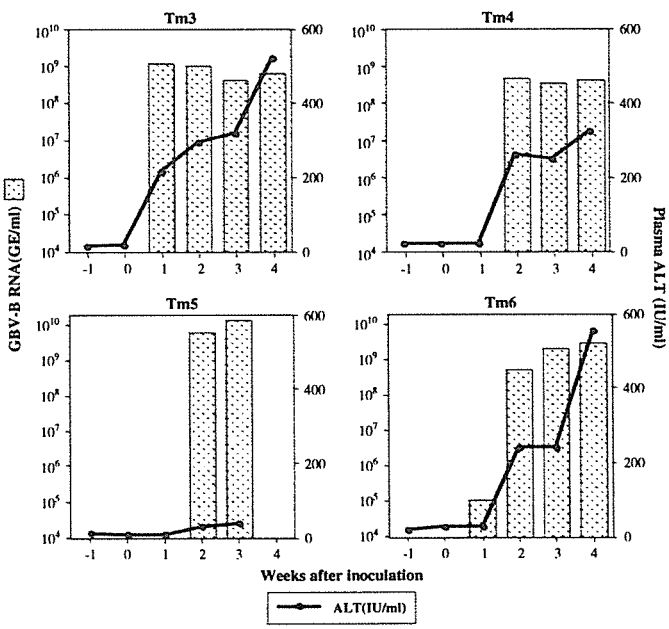

Fig. 2. Acute course of GBV-B infection in tamarins (Tm3 and Tm4) by *in vivo* passage of plasma (7.9×10^8 GE/head) obtained from the GBV-B RNA-inoculated Tm1 in comparison with GBV-B RNA transcript-inoculated tamarins (Tm5 and Tm6). The viral RNA copies and ALT levels in the plasma samples collected from each tamarin were indicated.

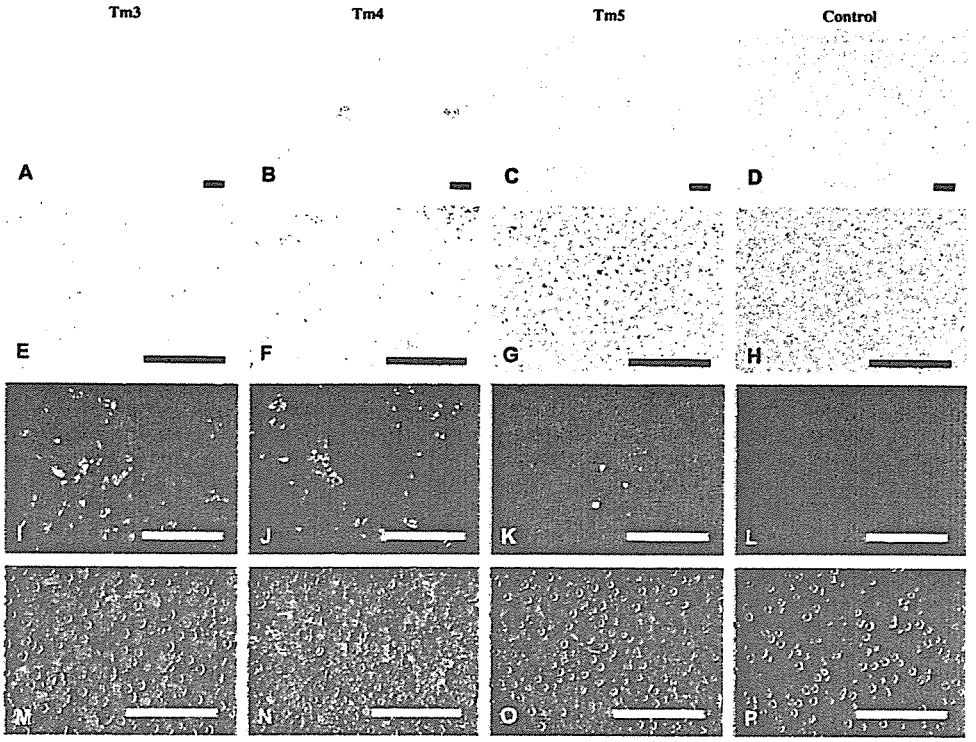

Fig. 3. Photomicrographs of liver sections from Tm3 (A, E, I, M), Tm4 (B, F, J, N), Tm5 (C, G, K, O), and an uninfected tamarin (D, H, L, P). A–H show sections with H&E staining, while I–L and M–P indicate sections with a TUNEL assay and immunohistochemistry for an active form of caspase-3, respectively. Sections immunostained for an active form of caspase-3 (green fluorescent) were counterstained with DAPI (blue fluorescent). Scale bars: 100 μm.

4. Discussion

GBV-B is most closely related to HCV and induces acute resolving hepatitis in tamarins. It is therefore reasonable that GBV-B has been considered to be a hepatotropic virus; in this study, however, we show for the first time that GBV-B is a pleiotropic virus and can disseminate to not only liver but also a variety of extrahepatic tissues such as hematolymphoid and genital tissues. Of note, there is ample evidence that persistent HCV infection manifests a variety of extrahepatic diseases, at least in part due to the extrahepatic tropisms of HCV (for review see [1]). This also suggests that extrahepatic tissues may serve as alternative reservoirs for HCV, while further analyses should still be required to understand the viral dynamics *in vivo*. Considering the similar pleiotropism of HCV and GBV-B, our results support and extend the usefulness of New World primates infected with GBV-B as a surrogate model for the study of pathogenesis and tropism of HCV infection.

Tamarins infected with GBV-B generally develop semi-acute viremia, of which peak levels regularly ranged from 10^7 to 10^9 GE/ml on the basis of previous reports [2,5,6,14,15]. From this point of view, the peal viremia (1.3×10^{10} GE/ml) in Tm5 euthanized at the acute phase of the viral infection appeared to be much greater than other cases. It seems likely that in Tm5 the lymphoid tissues but not liver were responsible for the highly efficient viral production, because (i)

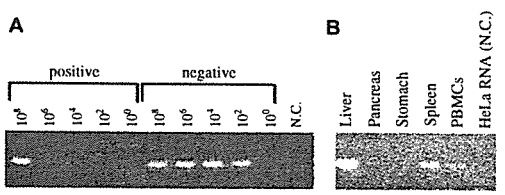

Fig. 4. (A) Titration of synthetic GBV-B RNA transcripts. Synthetic RNA transcripts corresponding to the positive- and negative-strands of part of the GBV-B were serially diluted and each transcript was subjected to amplification using strand-specific RT–PCR to determine the specificity and sensitivity of the assays. (B) Detection of negative-strand GBV-B RNA from various tissues. One microgram of total RNA obtained from tissues or cells was subjected to RT–PCR.

viral titer in the liver was lowest among three monkeys, which was consistent with minimal plasma ALT level and liver damage; (ii) yet, Tm5 exhibited highest viremia levels, (iii) the viral RNA levels in PBMCs, spleen and inguinal and intestinal lymph nodes of Tm5 were much greater than others, and (iv) we could detect negative-strand GBV-B RNA from not only liver but also spleen and PBMCs. Supposing that the entire virus in Tm3 plasma (3.8×10^8 GE/ml) was produced in the liver of which RNA titer was highest among tamarins, most of the virus in Tm5 plasma (1.3×10^{10} GE/ml) should be derived from extrahepatic tissues. Taken together, our data demonstrate preferential dissemination of GBV-B in extrahepatic tissues. In order to further define the cell type(s) in which GBV-B replicates efficiently, *in situ* histological analysis should be needed as indicated in the case of HCV [16].

It was possible that differential lymphotropism among GBV-B-infected tamarins could be due to adaptive mutation in the viral genome. From this point of view, we cloned the viral RNA obtained from plasma and liver; however, we did not find any sequence heterogeneity in the viral genome (data not shown). Furthermore, challenge of Tm5 plasma to naïve tamarins developed typical semi-acute hepatitis with regular viremia and did not reproduce the preferential lymphotropism (data not shown). These results indicate that GBV-B intrinsically has pleiotropism in a host-dependent manner. It is possible that multiple surface molecules in the host cells, which act as alternative receptors, would determine the pleiotropism of GBV-B. It remains to be investigated whether host molecules which are used as receptors for HCV [17] would also be used by GBV-B.

Histopathological studies showed the inflammatory responses in Tm3 and Tm4 livers; especially, the Tm4 liver developed strong degenerative changes, which was consistent with high ALT levels (Fig. 2G,H). Furthermore, the livers of Tm3 and Tm4 showed substantial proportions of apoptotic cells as revealed by greater signals of DNA fragmentation and caspase-3 activation, both of which were popular markers of apoptosis, than those in Tm5 (Fig. 3). It needs to be clarified whether such cytopathic effects could be directly induced by GBV-B infection into hepatocytes or whether effector cytotoxic T lymphocytes would be responsible for the cytopathicity.

Acknowledgments

We are grateful to Dr. Jens Bukh for providing pGBB. We also thank Mami Matsuda, Makiko Yahata and Tetsu Shimoji for technical assistance and members of Corporation for Production and Research of Laboratory Primates for the handling and care of the monkeys. This work was supported by a Health and Labour Science Research Grant from the Ministry of Health, Labour, and Welfare, Japan, and from New Energy and Industrial Technology Development Organization (NEDO) of Japan.

References

[1] V. Agnello, F.G. De Rosa, Extrahepatic disease manifestations of HCV infection, J. Hepatol. 40 (2004) 341–352.
[2] J. Bukh, C.L. Apgar, M. Yanagi, Toward a surrogate model for hepatitis C virus: An infectious molecular clone of the GB virus-B hepatitis agent, Virology 262 (1999) 470–478.
[3] A.S. Muerhoff, et al., Genomic organization of GB viruses A and B: two members of the Flaviviridae associated with GB agent hepatitis, J. Virol. 69 (1996) 5621–5630.
[4] J.N. Simons, et al., Identification of two flavivirus-like genomes in the GB hepatitis agent, Proc. Natl. Acad. Sci. USA. 92 (1995) 3401–3405.
[5] A. Martin, F. Bodola, D.V. Sangar, K. Goettge, V. Popov, R. Rijnbrand, R.E. Lanford, S.M. Lemon, Chronic hepatitis associated with GB virus B persistence in a tamarin after intrahepatic inoculation of synthetic viral RNA, Proc. Natl. Acad. Sci. USA. 100 (2003) 9962–99627.
[6] J.H. Nam, K. Faulk, R.E. Engle, S. Govindarajan, M. St Claire, J. Bukh, In vivo analysis of the 3′ untranslated region of GB virus B after in vitro mutagenesis of an infectious cDNA clone: persistent infection in a transfected tamarin, J. Virol. 78 (2004) 9389–9399.
[7] J.R. Jacob, K.C. Lin, B.C. Tennant, K.G. Mansfield, GB virus B infection of the common marmoset (*Callithrix jacchus*) and associated liver pathology, J. Gen. Virol. 85 (2004) 2525–2533.
[8] B. Beames, D. Chavez, B. Guerra, L. Notvall, K.M. Brasky, R.E. Lanford, Development of a primary tamarin hepatocyte culture system for GB virus-B: a surrogate model for hepatitis C virus, J. Virol. 74 (2000) 11764–11772.
[9] T.J. Pilot-Matias, A.S. Muerhoff, J.N. Simons, T.P. Leary, S.L. Buijk, M.L. Chalmers, J.C. Erker, G.J. Dawson, S.M. Desai, I.K. Mushahwar, Identification of antigenic regions in the GB hepatitis viruses GBV-A, GBV-B, and GBV-C, J. Med. Virol. 48 (1996) 329–338.
[10] K. Tsukiyama-Kohara, N. Iizuka, M. Kohara, A. Nomoto, Internal ribosome entry site within hepatitis C virus RNA, J. Virol. 66 (1992) 1476–1483.
[11] R.L. Chaves, J. Graff, A. Normann, B. Flehmig, Specific detection of minus strand hepatitis A virus RNA by Tail-PCR following reverse transcription, Nucleic Acids Res. 22 (1994) 1919–1920.
[12] J. Mellor, G. Haydon, C. Blair, W. Livingstone, P. and Simmonds, Low level or absent in vivo replication of hepatitis C virus and hepatitis G virus/GB virus C in peripheral blood mononuclear cells, J. Gen. Virol. 79 (1998) 705–714.
[13] H. Akari, S. Bour, S. Kao, A. Adachi, K. Strebel, The human immunodeficiency virus type 1 accessory protein Vpu induces apoptosis by suppressing the nuclear factor kappaB-dependent expression of antiapoptotic factors, J. Exp. Med. 194 (2001) 1299–1311.
[14] A. Sbardellati, E. Scarselli, E. Verschoor, A. De Tomassi, D. Lazzaro, C. Traboni, Generation of infectious and transmissible virions from a GB virus B full-length consensus clone in tamarins, J. Gen. Virol. 82 (2001) 2437–2448.
[15] R.E. Lanford, D. Chavez, L. Notvall, K.M. Brasky, Comparison of tamarins and marmosets as hosts for GBV-B infections and the effect of immunosuppression on duration of viremia, Virology 311 (2003) 72–80.
[16] E.J. Gowans, Distribution of markers of hepatitis C virus infection throughout the body, Semin. Liver Dis. 20 (2000) 85–102.
[17] L. Cocquerel, C. Voisset, J. Dubuisson, Hepatitis C virus entry: potential receptors and their biological functions, J. Gen. Virol. 87 (2006) 1075–1084.

Journal of General Virology (2006), 87, 1935–1945 DOI 10.1099/vir.0.81701-0

Non-structural protein 4A of *Hepatitis C virus* accumulates on mitochondria and renders the cells prone to undergoing mitochondria-mediated apoptosis

Yuki Nomura-Takigawa,[1] Motoko Nagano-Fujii,[1] Lin Deng,[1] Sohei Kitazawa,[2] Satoshi Ishido,[1]† Kiyonao Sada[1] and Hak Hotta[1]

Correspondence
Hak Hotta
hotta@kobe-u.ac.jp

Divisions of Microbiology[1] and Molecular Pathology[2], Kobe University Graduate School of Medicine, 7-5-1 Kusunoki-cho, Chuo-ku, Kobe 650-0017, Japan

Non-structural protein 4A (NS4A) of *Hepatitis C virus* (HCV) functions as a cofactor for NS3 by forming a complex with it to augment its enzymic activities. NS4A also forms a complex with other HCV proteins, such as NS4B/NS5A, to facilitate the formation of the viral RNA replication complex on the endoplasmic reticulum (ER) membrane. In addition to its essential role in HCV replication, NS4A is thought to be involved in viral pathogenesis by affecting cellular functions. In this study, it was demonstrated that NS4A was localized not only on the ER, but also on mitochondria when expressed either alone or together with NS3 in the form of the NS3/4A polyprotein and in the context of HCV RNA replication in Huh7 cells harbouring an HCV RNA replicon. Moreover, NS4A expression altered the intracellular distribution of mitochondria significantly and caused mitochondrial damage, as evidenced by the collapsed mitochondrial transmembrane potential and release of cytochrome *c* into the cytoplasm, which led ultimately to induction of apoptosis through activation of caspase-3, but not caspase-8. Consistently, Huh7 cells expressing NS3/4A and those harbouring an HCV RNA replicon were shown to be more prone to undergoing actinomycin D-induced, mitochondria-mediated apoptosis, compared with the control Huh7 cells. Taken together, these results suggest the possibility that HCV exerts cytopathic effect (CPE) on the infected cells under certain conditions and that NS4A is responsible, at least in part, for the conditional CPE in HCV-infected cells.

Received 19 November 2005
Accepted 22 February 2006

INTRODUCTION

Hepatitis C virus (HCV), a member of the family *Flaviviridae*, has a single-stranded, positive-sense RNA of about 9·6 kb in length. The virus genome encodes a precursor polyprotein of about 3000 aa, which is cleaved into at least 10 mature viral proteins, such as Core, E1, E2, p7, NS2, NS3, NS4A, NS4B, NS5A and NS5B (Reed & Rice, 2000). HCV is known to evade the host-defence mechanisms to establish persistent infection, causing chronic hepatitis, liver cirrhosis and hepatocellular carcinoma (Kiyosawa *et al.*, 1990; Tong *et al.*, 1995). It has been suggested that liver-cell injuries, either apoptotic or necrotic changes, are mediated principally by antiviral immune responses, such as HCV-specific cytotoxic T lymphocytes. However, the possible involvement of viral cytopathic effect (CPE) should also be taken into consideration.

Apoptosis involves two major pathways: the Fas-mediated pathway and the mitochondria-mediated pathway (Ashkenazi & Dixit, 1998; Gewies *et al.*, 2000). Fas-mediated apoptosis is conducted through facilitation of caspase-8 activation. Regarding HCV infection, Core was shown to induce Fas-mediated and tumour necrosis factor (TNF) receptor-mediated apoptosis (Ruggieri *et al.*, 1997). On the other hand, a number of apoptosis-inducing signals are concentrated at mitochondria to facilitate the release of cytochrome *c* from mitochondria, which induces formation of an apoptosome complex that includes apoptosis protease-activating factor-1 (Apaf-1) and procaspase-9 (Deveraux *et al.*, 1998; Fearnhead *et al.*, 1998; Gross *et al.*, 1999; Skulachev, 1998). This results in the activation of caspases and finally the cleavage of chromosomal DNA. Thus, mitochondria are intensive and central organelles regulating apoptotic signals.

A wide variety of viral proteins have been shown to localize specifically on mitochondria, such as cytomegalovirus vMIA (Goldmacher *et al.*, 1999), myxoma virus M11L (Everett *et al.*, 2002), Kaposi's sarcoma-associated herpesvirus K7 (Feng *et al.*, 2002; Wang *et al.*, 2002), human

†Present address: Laboratory for Infectious Immunity, RIKEN Research Center for Allergy and Immunology, 1-7-22 Suehiro-cho, Tsurumi-ku, Yokohama, Kanagawa 230-0045, Japan.

immunodeficiency virus type 1 Vpr (Jacotot *et al.*, 2000, 2001), human T-cell leukemia virus type 1 $p13^{II}$ (D'Agostino *et al.*, 2002), influenza virus PB1-F2 (Chen *et al.*, 2001), hepatitis B virus X protein (Rahmani *et al.*, 2000) and HCV Core (Schwer *et al.*, 2004). Some of them exert anti-apoptotic effects, and the others pro-apoptotic ones, by binding to apoptosis-regulating host-cell factors.

HCV NS4A is a non-structural protein of about 7 kDa that consists of 54 aa with a hydrophobic N-terminal region and a hydrophilic C terminus. NS4A is known to function as a cofactor for NS3 to augment its enzymic activities, such as serine protease (Failla *et al.*, 1995; Reed & Rice, 2000; Satoh *et al.*, 1995) and RNA and DNA helicases (Kuang *et al.*, 2004; Pang *et al.*, 2002; Reed & Rice, 2000). NS3 and NS4A, together with the other non-structural proteins, are incorporated into the HCV RNA replication complex, which is localized primarily on the endoplasmic reticulum (ER) and related membrane structures (Aizaki *et al.*, 2004; Egger *et al.*, 2002; Gosert *et al.*, 2003; Kim *et al.*, 1999; Wölk *et al.*, 2000). Little is known, however, about the possible effect(s) of NS4A on cellular functions, except for a few studies, including ours, showing that NS4A markedly inhibits the translation of the host cell (Florese *et al.*, 2002; Kato *et al.*, 2002).

In this study, we report that NS4A is localized not only on the ER, but also on mitochondria, and that NS4A induces apoptosis through a mitochondria-mediated pathway, as demonstrated by the decreased mitochondrial transmembrane potential, the release of cytochrome *c* from mitochondria and the activation of caspase-3, followed by the morphological changes characteristic of apoptotic cell death. We have also observed that Huh7 cells harbouring an HCV subgenomic RNA replicon are more prone to apoptosis than are control cells when treated with mitochondria-mediated apoptosis-inducing reagents, such as actinomycin D and staurosporine. These results collectively suggest the possibility that NS4A is one of the viral factors that induces CPE under certain conditions.

METHODS

Construction of expression plasmids. A cDNA fragment encoding the full-length NS4A of HCV subtype 1b (Con1 strain) was amplified by PCR from pFK5B2884Gly (a kind gift from Dr R. Bartenschlager, University of Heidelberg, Heidelberg, Germany) (Lohmann *et al.*, 2001). The amplified fragment was digested with *Eco*RI and subcloned into the unique *Eco*RI site of pSG5 (Stratagene) to generate pSG5-NS4A. Plasmids to express FLAG-tagged full-length NS4A and a C-terminally deleted mutant were constructed as reported previously with minor modifications (Florese *et al.*, 2002; Taguchi *et al.*, 2004). Other pSG5-based expression plasmids, such as pSG5-Core, -NS3, -NS4B, -NS3/4A, -NS5A and -NS5B, were described elsewhere (Deng *et al.*, 2006; Florese *et al.*, 2002; Ishido *et al.*, 2000; Song *et al.*, 1999; Wang *et al.*, 2000).

Cell culture and transfection. Huh7 cell lines harbouring an HCV subgenomic RNA replicon (Huh7-FK2884Gly-1 cells) that expresses NS3 to NS5B were reported previously (Lohmann *et al.*, 2001; Taguchi *et al.*, 2004; Takigawa *et al.*, 2004). The parental Huh7 cells served as a control. For transient expression of each HCV protein, Huh7 cells were transfected with an expression plasmid by using FuGENE 6 transfection reagent (Roche Diagnostics).

Cell-viability assay. Cells were seeded in 96-well plastic plates. Cell viability was determined based on mitochondrial NADH-dependent dehydrogenase activity by WST-1 assay using a sulfonated tetrazolium salt, 2-(4-iodophenyl)-3-(4-nitrophenyl)-5-(2,4-disulfophenyl)-2H-tetrazolium monosodium salt, as reported previously (Fujita *et al.*, 1996; Ishido *et al.*, 2000). A_{450} was read with a microplate photometer (Bio-Rad). Octuplicate cultures were prepared for each sample and the results were presented as a percentage of the value for untreated controls.

Subcellular fractionation. Cells (1×10^7) were harvested with a cell scraper and the cell suspension was centrifuged at 200 *g* for 5 min at 4 °C. The cells were resuspended in an ice-cold homogenization buffer containing 100 mM Tris/HCl (pH 8·0), 250 mM sucrose, 2 mM EDTA and protease inhibitors (Complete; Roche Molecular Biochemicals) and homogenized by using a homogenizer by 30 strokes at speed 4·4 of a motor-driven pestle (Wheaton overhead stirrer). The homogenate was centrifuged at 900 *g* for 10 min at 4 °C twice. Subsequently, the supernatant, deprived of the nuclei and unbroken cells, was centrifuged at 10 000 *g* for 10 min at 4 °C to collect mitochondria. The supernatant was further centrifuged at 100 000 *g* for 1 h and the pellet containing the ER was obtained. Each subcellular fraction was determined by immunoblotting with antibodies against protein disulfide isomerase (PDI) (Becton Dickinson) and mtHSP70 (Affinity BioReagents, Inc.) as markers for ER and mitochondria, respectively.

Immunoblotting. Cell lysates in a buffer containing 50 mM Tris/HCl (pH 6·8), 2 % SDS, 10 % glycerol and bromophenol blue were electrophoresed on 14–16 % SDS-polyacrylamide gels and transferred to nitrocellulose membranes as described previously (Muramatsu *et al.*, 1997). After being blocked with skimmed milk for 1 h at room temperature followed by washing with PBS containing 0·05 % Tween 20 (PBS-T), the membrane was incubated with an appropriate first antibody for 1 h, washed three times with PBS-T and incubated with a peroxidase-labelled second antibody at room temperature for 30 min. After being washed three times with PBS-T, the positive bands were visualized by using the ECL detection system (Amersham Biosciences) according to the manufacturer's instructions.

Immunofluorescence microscopy. Cells were fixed with 3·7 % formaldehyde for 10 min at room temperature and permeabilized with 0·1 % Triton X-100 for 10 min at room temperature. After being washed with PBS, the cells were incubated with a first antibody for 1 h, followed by washing three times with PBS-T and staining with a fluorescein isothiocyanate (FITC)-, Cy3- or Alexa Fluor 546-labelled second antibody. The first antibodies used were mouse mAbs against Core, NS3, NS4A and NS5A (kind gifts from Dr I. Yoshida, Research Institute for Microbial Diseases, Osaka University, Kan-Onji branch, Kagawa, Japan). The cells were washed again with PBS-T, mounted with 80 % glycerol and observed under a fluorescence microscope (Olympus) or a confocal immunofluorescence microscope (Carl Zeiss). MitoTracker (Molecular Probes) and pEYFP-Golgi (Clontech) were used for staining mitochondria and the Golgi apparatus, respectively.

Immunoelectron microscopy. Immunoelectron microscopy was performed as described previously with some modifications (Hidajat *et al.*, 2005). In brief, cells were fixed with 4 % paraformaldehyde and 1 % glutaraldehyde in 150 mM HEPES-KOH (pH 7·4) for 10 min at room temperature. The cells were collected by a cell scraper, centrifuged and dehydrated through a series of 50, 70, 80, 90 and 100 % ethanol. The sample was embedded in LR White resin (London Resin Co. Ltd) and kept at −20 °C for 2 days. After ultrathin

sectioning, sections were blocked with 0·5 % BSA solution and incubated with anti-NS4A mouse mAb for 1 h at room temperature. After being washed with PBS, the sections were incubated with goat anti-mouse IgG conjugated to 10 nm gold (Sigma) for 30 min at room temperature. After being washed with PBS and extra-pure water, the sections were dried, stained with lead citrate and observed under an electron microscope (JEM-1200EX; JOEL).

Mitochondrial transmembrane potential. Changes in the mitochondrial transmembrane potential were examined by using rhodamine 123 (Rho123; Sigma). Rho123, a fluorescent, lipophilic, cationic dye, accumulates in mitochondria of living cells and has been used for evaluating changes in the mitochondrial transmembrane potential (Davis *et al.*, 1985; Leprat *et al.*, 1990; Li *et al.*, 1999; Lin *et al.*, 2004). Cells (5×10^5) were washed with PBS and stained with a staining solution containing Rho123 (0·5 μg ml^{-1}) for 15 min at 37 °C. The fluorescence emitted from Rho123 was analysed by a flow cytometer (Becton Dickinson).

Caspase enzymic activity. Caspase-3 activity was measured by using Caspase-GloTM 3/7 reagent (Promega) according to the manufacturer's instructions. In brief, a proluminescent caspase-3/7 substrate, which contains the tetrapeptide sequence DEVD, was added to cells cultured on a microplate. The cells were incubated for 30 min at room temperature and the luminescence of each sample was measured by a microplate luminometer (Luminescencer-JNP AB-2100; ATTO). Caspase-8 activity was measured by using a FLICE/Caspase-8 colorimetric protease assay kit (Medical Biological Laboratories Co. Ltd) according to the manufacturer's instructions. Cells were detached from the dishes with trypsin and lysed in an ice-cold lysis buffer supplied with the kit for 10 min. The cytosolic extracts obtained were mixed with IETD-*p*NA, the substrate of caspase-8, and incubated for 2 h at 37 °C. A_{405} was read with a microplate photometer (Bio-Rad).

Cytological markers for apoptosis: morphological changes of the nuclei. Cells were fixed with 100 % methanol at −20 °C for 20 min, washed twice with PBS and stained with 10 μM Hoechst 33342 at room temperature for 10 min, as described previously (Fujita *et al.*, 1996; Ishido *et al.*, 2000). The morphology of the nuclei of the cells was examined under a light microscope.

RESULTS

NS4A is localized on mitochondria

We first examined the intracellular localization of NS4A. Immunofluorescence analysis revealed that NS4A colocalized with MitoTracker, a marker for mitochondria, in Huh7 cells using a transient-expression system (Fig. 1a, top). It should be noted that, in NS4A-expressing cells, mitochondria accumulated in the perinuclear region, exhibiting a doughnut-like appearance. NS4A was also localized at the ER to a considerable degree (Fig. 1a, middle) and, to a much lesser degree, at the Golgi apparatus (bottom). Mitochondrial localization of NS4A was observed when NS4A was co-expressed with NS3 *in cis* as well (Fig. 1b, top). We also tested the possible mitochondrial localization of the other HCV proteins, such as Core, NS3, NS4B and NS5A, and found that Core and NS5A were partially localized on mitochondria. Unlike NS4A, however, none of these HCV proteins altered the intracellular-distribution pattern of mitochondria. The mitochondrial localization of NS4A in Huh7 cells was confirmed by further experiments. Subcellular-fractionation analysis revealed that NS4A was detected abundantly in a mitochondrial fraction of Huh7 cells in a transient-expression system (Fig. 1c). Moreover, NS4A was detected in a mitochondrial fraction obtained from Huh7 cells harbouring an HCV subgenomic RNA replicon. PDI, an ER marker, was barely detected, if at all, in the mitochondrial fraction, with the result excluding the possible contamination of the mitochondrial fraction with the ER and thereby verifying the specificity of the mitochondrial localization of NS4A in those cells. Confocal immunofluorescence microscopic analysis revealed that NS4A was partially colocalized on mitochondria in Huh7 cells harbouring the HCV subgenomic RNA replicon, although to a lesser extent than that observed in cells expressing NS4A or NS3/4A transiently (Fig. 1d). Also, immunoelectron microscopic analysis demonstrated clearly that NS4A was localized on both ER and mitochondria of Huh7 cells expressing NS4A transiently (Fig. 1e) and those harbouring the HCV RNA replicon (Fig. 1f). The immunogold staining was not observed in the control cells without NS4A expression, ensuring the specificity of the staining (data not shown). From these results, we concluded that NS4A was localized preferentially on mitochondria. We also speculated that NS4A could potentially alter the intracellular distribution and functions of mitochondria.

NS4A induces cell death

While analysing the intracellular localization of NS4A, we noticed that NS4A-expressing cells exhibited severe cell damage after prolonged cultivation. In line with this observation, we could not generate any Huh7 cell line stably expressing NS4A (data not shown). We therefore examined the possible effect of NS4A on cell viability. The result demonstrated that NS4A caused cell death (Fig. 2). When NS4A was co-expressed with NS3 *in cis* (NS3/4A), cell death was not observed, although a comparable level of NS4A expression was achieved in these cells. These results suggest that, under these experimental conditions, the cell death-inducing effect of NS4A was abolished after forming a complex with NS3. This result, however, does not necessarily exclude the possibility that NS3/4A could affect cell death under certain conditions (see below).

NS4A induces the collapse of the mitochondrial transmembrane potential

To assess the molecular mechanism of NS4A-induced cell death, we first measured the mitochondrial transmembrane potential by using Rho123. In this analysis, Huh7 cells transiently transfected with the pSG5 vector and those treated with staurosporine served as a negative and a positive control, respectively. As shown in Fig. 3, a larger number of NS4A-expressing cells showed decreased mitochondrial transmembrane potential (24·0 %) compared with the non-expressing control (7·6 %) and cells expressing NS3 alone (10·5 %). Again, the mitochondria-damaging effect of NS4A was counteracted by NS3 (NS3/4A; 9·5 %).

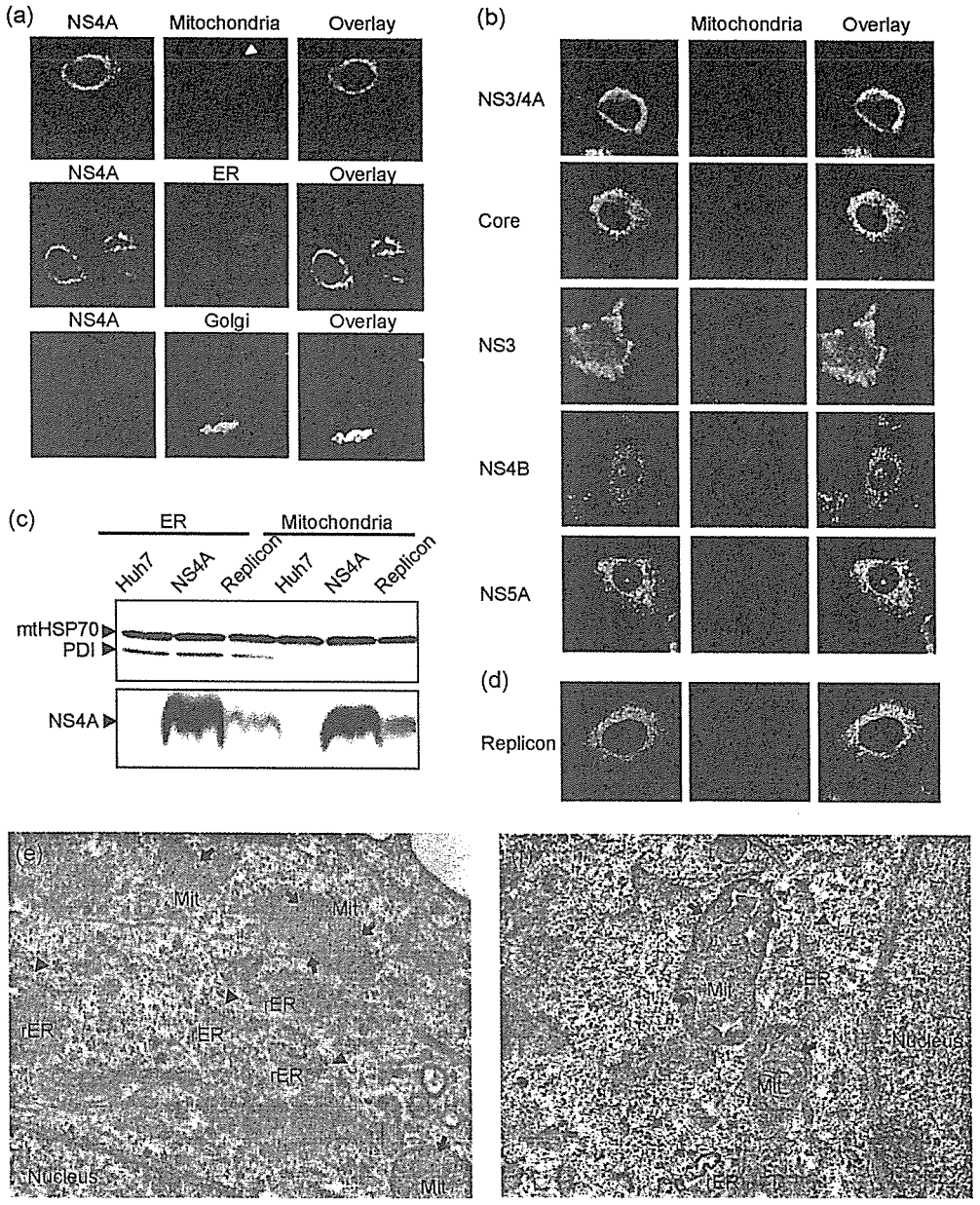

Fig. 1. Localization of NS4A on mitochondria. (a) Immunofluorescence analysis. Huh7 cells expressing NS4A transiently were double-stained with anti-NS4A mouse mAb (left panels) and MitoTracker Red (upper middle panel), anti-calregulin rabbit antiserum as an ER marker (centre) or pEYFP-Golgi (lower middle panel). Second antibodies used were either FITC-conjugated anti-mouse IgG (green), Cy3-conjugated anti-rabbit IgG (red) or Alexa Fluor 546-conjugated anti-mouse IgG (red). Overlaid pictures are shown on the right. Note a doughnut-like, perinuclear staining of mitochondria in NS4A-expressing cells (upper middle panel, arrowhead). (b) Huh7 cells transiently expressing NS3/4A were stained with anti-NS4A antibody plus FITC-conjugated anti-mouse IgG (left panel) and MitoTracker Red as a mitochondrial marker (centre). Also, cells expressing Core, NS3, NS4B and NS5A transiently were double-stained with specific antibodies (Core, NS3 and NS5A) or HCV-infected patient serum (NS4B) and MitoTracker Red. Second antibodies used were FITC-conjugated anti-mouse IgG or anti-human IgG. Overlaid pictures are shown on the right. (c) Subcellular fractionation. Huh7 cells expressing NS4A transiently, those harbouring an HCV subgenomic RNA replicon and the parental control were fractionated. The ER and mitochondrial fractions were probed with anti-NS4A antibody. The absence of ER in the mitochondrial fraction was confirmed by staining with antibodies against PDI. (d) Huh7 cells harbouring an HCV subgenomic RNA replicon were stained with anti-NS4A antibody plus FITC-conjugated anti-mouse IgG (left panel) and MitoTracker Red (centre). An overlaid picture is shown on the right. (e) Immunoelectron microscopic analysis of Huh7 cells expressing NS4A transiently. Arrows and arrowheads indicate NS4A localized at mitochondria and ER, respectively. (f) Immunoelectron microscopic analysis of Huh7 cells harbouring an HCV subgenomic RNA replicon. Arrows and arrowheads indicate NS4A localized at mitochondria and ER, respectively. Mit, Mitochondrion; rER, rough ER.

NS4A induces the release of cytochrome c from mitochondria

The collapse of the mitochondrial transmembrane potential would impair the intrinsic functions of mitochondria, triggering apoptosis and/or necrosis. Cytochrome *c* is normally present in the mitochondrial intermembrane space and is released to the cytosol when cells undergo apoptosis. We therefore examined whether expression of NS4A could trigger the release of cytochrome *c* from mitochondria. As had been expected, nearly 70 % of NS4A-expressing Huh7 cells, but not the empty vector-transfected control, showed the release of cytochrome *c* into the cytoplasm 48 h after transfection, as evidenced by diffuse staining of cytochrome *c* throughout the cell (Fig. 4a, b). Expression of Core (Fig. 4b), NS4B and NS5A (data not shown), but not NS3, each induced cytochrome *c* release only slightly (~10 %). Cells expressing NS3/4A did not induce cytochrome *c* release, but rather exhibited doughnut-like, perinuclear staining of cytochrome *c* (Fig. 4a, b). The absence of cytochrome *c* release in NS3/4A-expressing cells was confirmed even 96 h after transfection (data not shown). The doughnut-like staining pattern of NS4A closely resembled that of mitochondrial localization in cells expressing either NS4A alone or NS3/4A (Fig. 1a, b). These results collectively suggest the possibility that both NS4A by itself and the NS3/4A complex accumulate on mitochondria, but that they exert differential effects on the cellular conditions depending upon its molecular status.

Cytochrome *c* release was observed in cells expressing NS4AΔC14 (Fig. 4b). A comparable expression level of full-length NS4A and NS4AΔC14 was verified by immunoblotting. These results suggested that the C-terminal 14 residues of NS4A were not involved in the induction of cytochrome *c* release.

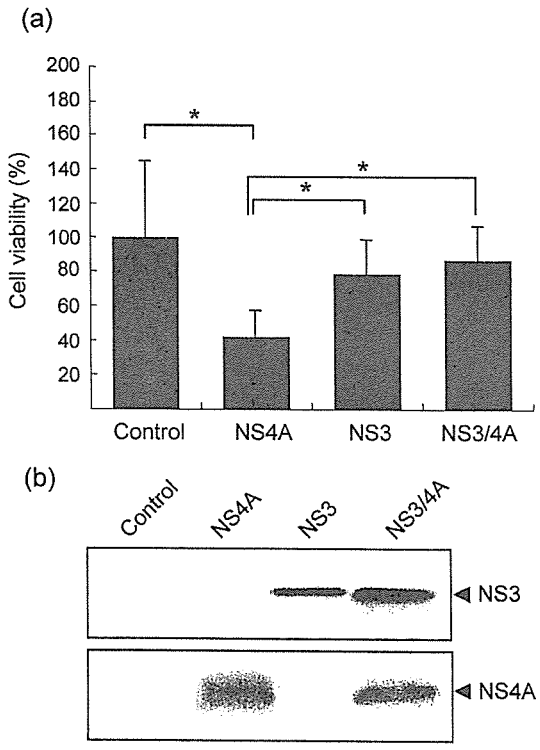

Fig. 2. (a) Cell death induced by NS4A. Huh7 cells expressing NS4A, NS3 and NS3/4A transiently for 48 h, as well as a vector-transfected, non-expressing control, were examined for cell viability by WST-1 assay. Cell viability of plasmid-harbouring cells was calculated. *$P<0{\cdot}01$ (Student's *t*-test). (b) Expression levels of NS3 and NS4A were determined by immunoblotting (bottom).

NS4A activates caspase-3, but not caspase-8, and induces apoptosis

Cytochrome *c*, once released to the cytosol, plays an important role in the activation of caspase-3, which is a principal effector for induction of apoptosis (Liu *et al.*, 1996). Consistent with this idea, we observed that caspase-3 activity was enhanced in NS4A-expressing Huh7 cells compared with the non-expressing control (Fig. 5a, left panel). On the other hand, caspase-8 was not activated by NS4A expression (Fig. 5a, right panel). Caspase-8 is known to be involved in the Fas-mediated apoptotic pathway (Muzio *et al.*, 1996; Shu *et al.*, 1997). NS4A-mediated cell death was inhibited almost completely by treatment with Z-VAD-fmk, a general inhibitor of caspases (Fig. 5b). These results collectively suggested that NS4A induced apoptosis through the mitochondria-mediated, but not the Fas-mediated, pathway.

To confirm that the NS4A-mediated cell death was due to apoptosis, the nuclei of the cells were stained with Hoechst 33342 and their morphology was examined. Chromatin condensation and nuclear fragmentation, typical cytological markers for apoptosis, were observed in NS4A-expressing cells as well as in staurosporine-treated, positive-control cells (Fig. 6a). A similar morphological change of the nucleus was also observed in NS3/4A-expressing cells more frequently than in the vector-transfected control (Fig. 6b). This result implies the possibility that the NS3/4A complex exerts certain effects on cell function, but that the possible effect on cell survival may not become evident in the absence of additional factor(s).

NS3/4A-expressing Huh7 cells are prone to undergoing mitochondria-mediated apoptosis

We hypothesized that the NS3/4A complex might direct the cells to a pre-apoptotic status that, upon exposure to an otherwise ineffective low dose of apoptotic stimuli, leads the cells to apoptosis. To examine this possibility, cells expressing NS3/4A or NS4A alone and the non-expressing control were treated with a suboptimal dose of actinomycin D (100 ng ml^{-1}) and cell viability was determined. The results obtained revealed that NS3/4A-expressing cells, as well as those expressing NS4A alone, were more prone to undergoing actinomycin D-induced (mitochondria-mediated)

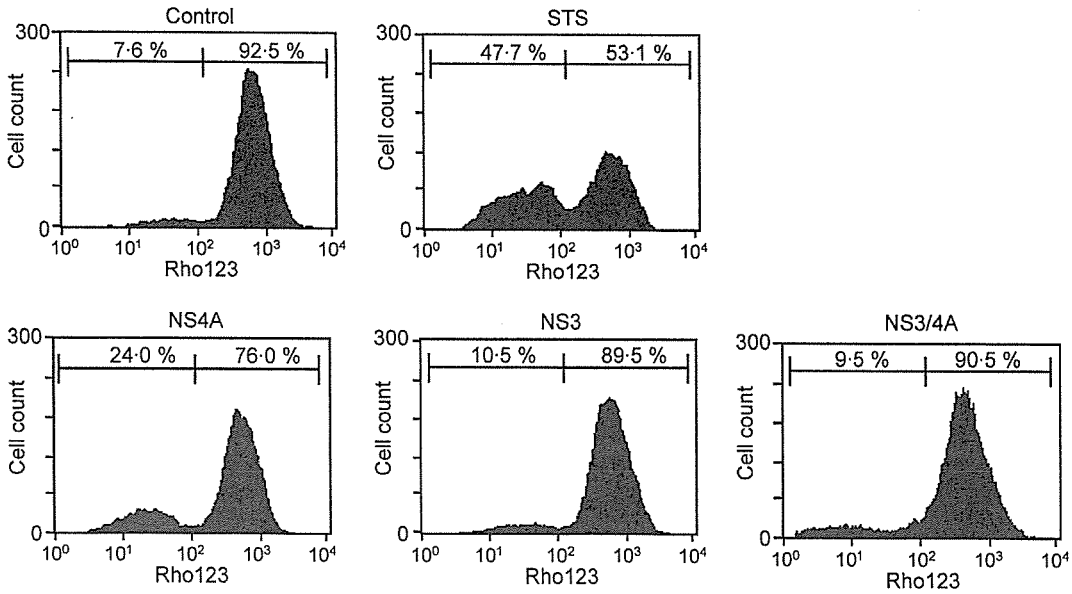

Fig. 3. Collapse of the mitochondrial transmembrane potential by NS4A. Huh7 cells expressing NS4A, NS3 and NS3/4A for 24 h transiently, as well as a vector-transfected, non-expressing control, were measured for the mitochondrial transmembrane potential by staining the cells with Rho123 followed by flow-cytometric analysis. Cells treated with staurosporine (STS, 1 μM) for 6 h served as a positive control. Reduced Rho123 staining indicates the mitochondrial transmembrane potential reduction.

apoptosis than the control cells (Fig. 6c). Similar results were obtained when the cells were treated with 50 ng actinomycin D ml^{-1} (data not shown).

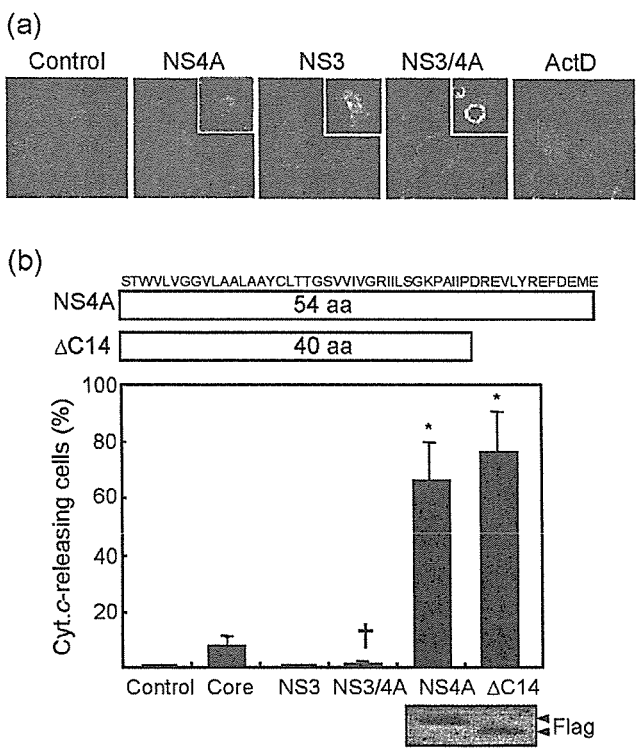

Fig. 4. Cytochrome *c* release from mitochondria into the cytoplasm by NS4A. (a) Huh7 cells expressing NS4A, NS3 and NS3/4A transiently for 48 h, as well as the vector-transfected, non-expressing control, were stained with anti-cytochrome *c* mouse mAb and Alexa Fluor 546-conjugated anti-mouse IgG. Expression of NS4A and NS3 was confirmed by staining the cells with HCV-infected patient serum that reacted strongly to NS4A and NS3, followed by FITC-conjugated anti-human IgG (right upper corner of the three panels). Cells treated with actinomycin D (ActD; 300 ng ml^{-1}) for 24 h served as a positive control. (b) Percentage of cells showing cytochrome *c* release among plasmid-harbouring cells. Huh7 cells expressing Core, NS3, NS3/4A, FLAG-tagged NS4A and FLAG-tagged NS4AΔC14 transiently, as well as the vector-transfected, non-expressing control, were tested. *$P<0{\cdot}01$ compared with the control (Student's *t*-test). †All of the NS3/4A-expressing cells showed perinuclear accumulation of cytochrome *c* staining (see Fig. 4a), which coincided with the mitochondrial-localization pattern, as evidenced by staining with a mitochondrial marker (MitoTracker). An equivalent expression level of FLAG-tagged NS4A and FLAG-tagged NS4AΔC14 was verified by immunoblotting (bottom).

Huh7 cells harbouring an HCV subgenomic RNA replicon are prone to undergoing mitochondria-mediated, but not Fas-mediated, apoptosis

In cells infected with HCV or those harbouring an HCV RNA replicon, NS4A is expressed in the context of virus replication, where NS4A is principally incorporated into the viral RNA replication complex together with other

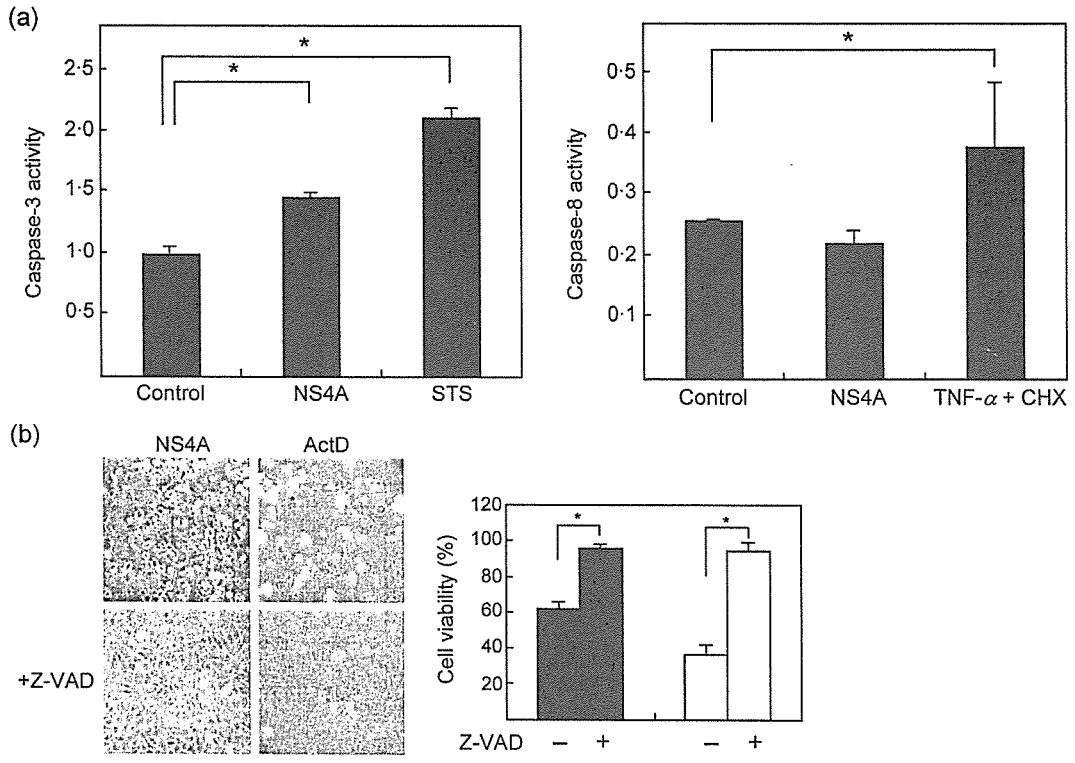

Fig. 5. Activation of caspase-3, but not caspase-8, by NS4A. (a) Huh7 cells expressing NS4A transiently for 24 h and a vector-transfected, non-expressing control were examined for caspase-3 (left panel) and caspase-8 (right panel) activities. Cells treated with staurosporine (STS, 1 μM) for 3 h and those treated with TNF-α (50 ng ml^{-1}) and cycloheximide (CHX, 5 μg ml^{-1}) for 6 h served as positive controls for caspase-3 and caspase-8 measurements, respectively. *$P<0·01$ (Student's *t*-test). (b) Inhibition of NS4A-induced cell death by a caspase inhibitor, Z-VAD-fmk. Huh7 cells expressing NS4A (left panels) and those treated with actinomycin D (ActD; 300 ng ml^{-1}) for 24 h (right panels) were cultured in the absence (upper panels) or presence of 20 μM Z-VAD-fmk (lower panels) and observed under an inverted microscope. Percentage of cell viability among plasmid-transfected cells was calculated and shown on the right (filled bars, NS4A; empty bars, ActD). *$P<0·01$ (Student's *t*-test).

non-structural proteins. We therefore examined whether Huh7 cells harbouring an HCV subgenomic RNA replicon are prone to undergoing apoptosis under some circumstances. As shown in Fig. 7(a), the replicon-harbouring cells underwent actinomycin D-induced (mitochondria-mediated) apoptosis to a significantly larger extent than that observed with the non-expressing control. On the other hand, no difference in the degree of TNF-α-induced apoptosis was observed between the replicon-harbouring cells and the control Huh7 cells. Similar results were obtained reproducibly with two other independent clones harbouring the same HCV RNA replicon (data not shown). The collapse of the mitochondrial transmembrane potential was significantly more evident in the replicon-harbouring cells (35·7%) than in the control (10·0%) when treated with actinomycin D (Fig. 7b).

DISCUSSION

HCV infection in the liver causes apoptotic and/or necrotic cell death of hepatocytes. The cell death is thought to be mediated principally by HCV-specific cytotoxic T cells; however, direct CPE by the virus itself should not be overlooked. Many viruses, including HCV, possess viral proteins that either promote or inhibit cell death. Among HCV proteins, Core (Sacco *et al.*, 2003), NS2 (Erdtmann *et al.*, 2003), NS3 (Fujita *et al.*, 1996) and NS5A (He *et al.*, 2002; Lan *et al.*, 2002) have been reported to possess anti-apoptotic functions. Also, there are reports showing that Core (Hahn *et al.*, 2000; Moorman *et al.*, 2003; Ruggieri *et al.*, 1997, 2003; Soguero *et al.*, 2002; Zhu *et al.*, 2001), E1 (Ciccaglione *et al.*, 2003, 2004), NS3/4A (Hsu *et al.*, 2003), NS5A and NS5B (Siavoshian *et al.*, 2005) function as pro-apoptotic proteins.

NS4A is known to localize in the ER (Mottola *et al.*, 2002; Reed & Rice, 2000). On the other hand, we demonstrate in the present study that NS4A was localized not only in the ER, but also on mitochondria (Fig. 1). Normally, mitochondria take a filamentous form, with a minor fraction exhibiting a micropunctate appearance, and are distributed evenly in the cell. In NS4A-expressing cells, however, mitochondria took

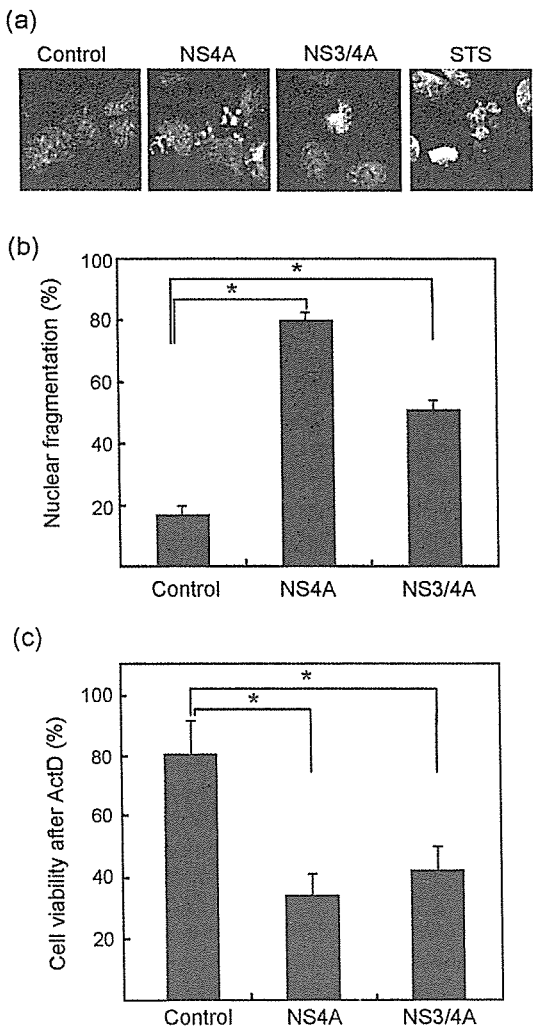

Fig. 6. Evidence for NS4A-induced apoptosis. (a) Huh7 cells expressing NS4A and NS3/4A transiently for 48 h and the vector-transfected, non-expressing control were stained with Hoechst 33342 (10 μM) for 10 min and observed under a fluorescent microscope. Cells treated with staurosporine (STS, 1 μM) for 6 h served as a positive control. (b) Percentage of cells showing nuclear fragmentation was calculated. $^*P<0{\cdot}01$ (Student's *t*-test). (c) Huh7 cells expressing NS4A or NS3/4A transiently and the vector-transfected, non-expressing control were treated with a suboptimal dose of actinomycin D (100 ng ml^{-1}) for 24 h and cell viability was determined.

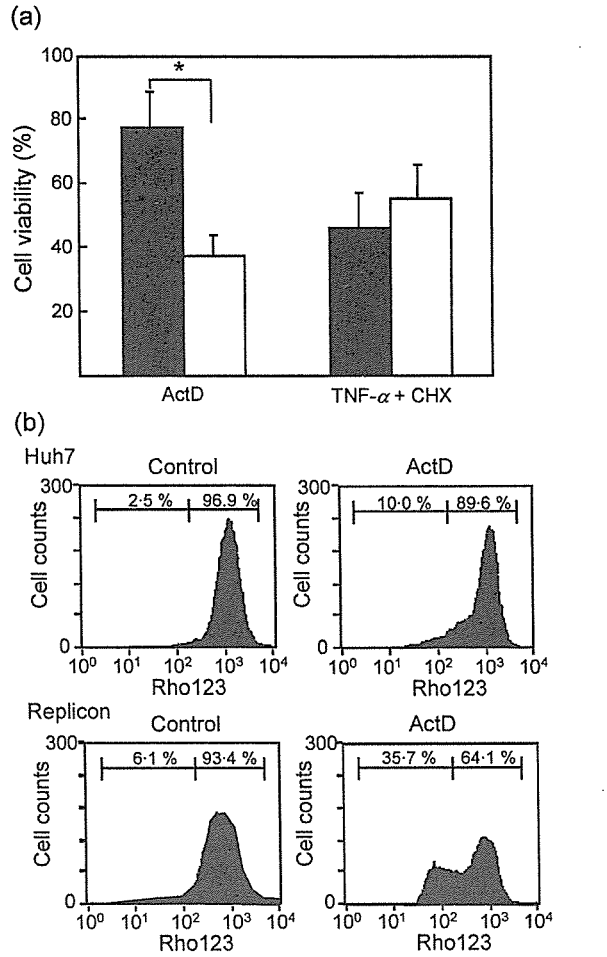

Fig. 7. Increased sensitivity of HCV RNA replicon-harbouring cells to mitochondria-mediated, but not TNF-α-receptor-mediated, apoptotic stimuli. (a) Huh7 cells harbouring an HCV subgenomic RNA replicon (empty bars) and the parental control (filled bars) were left untreated or treated with either actinomycin D (ActD, 100 ng ml^{-1}) for 24 h or TNF-α (50 ng ml^{-1}) and cycloheximide (CHX, 5 μg ml^{-1}) for 9 h. Cell viability was measured by WST-1 assay. $^*P<0{\cdot}01$ (Student's *t*-test). (b) The cells in (a) were analysed for mitochondrial transmembrane potential by using Rho123. Reduced Rho123 staining indicates the mitochondrial transmembrane potential reduction.

a dumpy form and were aggregated in the perinuclear region, exhibiting a doughnut-like appearance (Fig. 1a). Similar perinuclear accumulation of mitochondria was observed also in NS3/4A-expressing cells (Fig. 4a; data not shown). These results suggest the possibility that NS4A, either expressed alone or co-expressed with NS3 so as to form a complex with it, accumulates on mitochondria. The next question that we raised was what would be the consequence of NS4A accumulation on mitochondria. In this regard, we found that NS4A induced mitochondrial transmembrane potential reduction (Fig. 3) and the release of cytochrome *c* into the cytoplasm (Fig. 4). Expression levels of Bax and Bcl-2 were not affected by NS4A or NS3/4A (data not shown), suggesting that a Bax/Bcl-2 imbalance was unlikely to be the cause of the observed mitochondrial damage. The molecular event(s) triggering the mitochondrial damage is/are currently unknown. In any case, cytochrome *c* is usually bound to the inner mitochondrial membrane through an association with the anionic phospholipid cardiolipin. The release of cytochrome *c* from mitochondria triggers the formation of an apoptosome complex that includes Apaf-1, procaspase-9 and ATP, leading to the activation of caspases and eventually apoptosis of the cell. Consistent with this scenario, we

observed NS4A-induced caspase-3 activation (Fig. 5a) and cell death (Fig. 2), the latter of which was blocked by a broad-spectrum caspase inhibitor Z-VAD (Fig. 5b). NS4A-expressing cells exhibited nuclear fragmentation (Fig. 6), which is considered as an apoptosis marker. On the other hand, NS4A did not induce caspase-8 activation (Fig. 5a). It is well-known that caspase-8 is activated upon Fas- and TNF-α-receptor-mediated apoptosis (Muzio *et al.*, 1996; Shu *et al.*, 1997). These results collectively suggest that NS4A induces mitochondria-mediated, but not Fas- or TNF-α-mediated, apoptosis.

NS4A consists of 54 aa, with its N-terminal and central regions being hydrophobic (Failla *et al.*, 1995). Deletion mutational analysis revealed that a C-terminally deleted mutant (NS4AΔC14) also induced the release of cytochrome *c* (Fig. 4b). In this regard, we previously observed that NS4AΔC14 (aa 1–40), but not NS4AΔN17 (aa 18–54) or NS4AΔN17ΔC14 (aa 18–40), inhibited the translation in the cell (Florese *et al.*, 2002). These results imply an important role for the N-terminal hydrophobic region of NS4A in affecting host cellular functions. On the other hand, NS4A is known to bind to NS3 and NS4B/NS5A through its hydrophobic central region. Our results showed that the NS4A-induced apoptosis and reduction in the mitochondrial transmembrane potential were alleviated by NS3 (Figs 2–4). It should be emphasized, however, that the mitochondrial morphology and intracellular localization (Fig. 4a) and the nuclear morphology (Fig. 6a, b) were altered in NS3/4A-expressing cells. This result implies the possibility that the NS3/4A complex, after being transported to mitochondria by virtue of NS4A, exerts a significant effect on mitochondrial function, and possibly even other cellular functions, without affecting mitochondrial transmembrane potential. In fact, we observed that NS3/4A-expressing cells were more sensitive to actinomycin D-induced, mitochondria-mediated apoptosis than the non-expressing control (Fig. 6c). It is not surprising that a virus can mediate mitochondrial dysfunction through a number of different mechanisms. It has recently been reported that NS3/4A cleaves the mitochondrial antiviral signalling protein, MAVS, thereby inhibiting the retinoic acid-inducible gene I-mediated induction of beta interferon production (Li *et al.*, 2005). It is possible that NS3/4A cleaves another mitochondrial protein(s) to modulate mitochondria-mediated cellular activities.

The possible mitochondria-damaging effect of NS4A alone might be weakened in HCV-infected cells, where NS4A is incorporated into the RNA replication complex with NS3, NS4B, NS5A and NS5B. It may explain why HCV RNA replicon-harbouring cells grew well under normal conditions, despite the apoptosis-inducing function of NS4A. Upon receiving a suboptimal degree of apoptotic stimuli, however, Huh7 cells harbouring an HCV subgenomic RNA replicon underwent apoptosis to a larger extent than HCV replicon-free control cells (Fig. 7). This result suggests the possibility that HCV infection renders host cells more sensitive to mitochondria-mediated apoptosis. This notion is in line with previous observations that, in hepatocytes of HCV-infected patients, mitochondria exhibited irregular and dumpy appearances with thin and fragmented cristae (Barbaro *et al.*, 1999) and that hepatocytes of HCV-infected patients underwent apoptosis *in vivo* (Bantel *et al.*, 2001; Bantel & Schulze-Osthoff, 2003; Hayashi *et al.*, 1997; Hiramatsu *et al.*, 1994). HCV-induced apoptosis was also observed in B-cell lymphoma cells *in vitro* (Sung *et al.*, 2003). It should be mentioned that, after receiving a pro-apoptotic stimulus, such as calcium ionophore treatment, cells undergo either apoptosis or necrosis depending upon the amount of ATP available in the microenvironment (Eguchi *et al.*, 1997). Therefore, HCV infection may induce necrosis as well under some conditions. In conclusion, our present data imply the possibility that NS4A is responsible, at least partly, for conditional cell death (CPE) of hepatocytes in HCV-infected patients.

ACKNOWLEDGEMENTS

The authors are grateful to Dr R. Bartenschlager (University of Heidelberg, Heidelberg, Germany) for providing an HCV subgenomic RNA replicon (pFK5B2884Gly). Thanks are also due to Dr I. Yoshida (Research Institute for Microbial Diseases, Osaka University, Kan-Onji Branch, Kagawa, Japan) for providing mouse mAbs against HCV NS3, NS4A and NS5A. This work was supported in part by Grants-in-Aid for Scientific Research from the Ministry of Education, Culture, Sports, Science and Technology, the Japan Society for the Promotion of Science and the Ministry of Health, Labour and Welfare, Japan. This study was also carried out as part of the 21COE Program at Kobe University Graduate School of Medicine.

REFERENCES

Aizaki, H., Lee, K.-J., Sung, V. M.-H., Ishiko, H. & Lai, M. M. C. (2004). Characterization of the hepatitis C virus RNA replication complex associated with lipid rafts. *Virology* **324**, 450–461.

Ashkenazi, A. & Dixit, V. M. (1998). Death receptors: signaling and modulation. *Science* **281**, 1305–1308.

Bantel, H. & Schulze-Osthoff, K. (2003). Apoptosis in hepatitis C virus infection. *Cell Death Differ* **10**, S48–S58.

Bantel, H., Lügering, A., Poremba, C., Lügering, N., Held, J., Domschke, W. & Schulze-Osthoff, K. (2001). Caspase activation correlates with the degree of inflammatory liver injury in chronic hepatitis C virus infection. *Hepatology* **34**, 758–767.

Barbaro, G., Di Lorenzo, G., Asti, A., Ribersani, M., Belloni, G., Grisorio, B., Filice, G. & Barbarini, G. (1999). Hepatocellular mitochondrial alterations in patients with chronic hepatitis C: ultrastructural and biochemical findings. *Am J Gastroenterol* **94**, 2198–2205.

Chen, W., Calvo, P. A., Malide, D. & 10 other authors (2001). A novel influenza A virus mitochondrial protein that induces cell death. *Nat Med* **7**, 1306–1312.

Ciccaglione, A. R., Marcantonio, C., Costantino, A., Equestre, M. & Rapicetta, M. (2003). Expression of HCV E1 protein in baculovirus-infected cells: effects on cell viability and apoptosis induction. *Intervirology* **46**, 121–126.

Ciccaglione, A. R., Marcantonio, C., Tritarelli, E., Equestre, M., Magurano, F., Costantino, A., Nicoletti, L. & Rapicetta, M. (2004).

The transmembrane domain of hepatitis C virus E1 glycoprotein induces cell death. *Virus Res* **104**, 1–9.

D'Agostino, D. M., Ranzato, L., Arrigoni, G. & 10 other authors (2002). Mitochondrial alterations induced by the p13^{II} protein of human T-cell leukemia virus type 1. *J Biol Chem* **277**, 34424–34433.

Davis, S., Weiss, M. J., Wong, J. R., Lampidis, T. J. & Chen, L. B. (1985). Mitochondrial and plasma membrane potentials cause unusual accumulation and retention of rhodamine 123 by human breast adenocarcinoma-derived MCF-7 cells. *J Biol Chem* **260**, 13844–13850.

Deng, L., Nagano-Fujii, M., Tanaka, M., Nomura-Takigawa, Y., Ikeda, M., Kato, N., Sada, K. & Hotta, H. (2006). NS3 protein of *Hepatitis C virus* associates with the tumour suppressor p53 and inhibits its function in an NS3 sequence-dependent manner. *J Gen Virol* **87**, 1703–1713.

Deveraux, Q. L., Roy, N., Stennicke, H. R., Van Arsdale, T., Zhou, Q., Srinivasula, S. M., Alnemri, E. S., Salvesen, G. S. & Reed, J. C. (1998). IAPs block apoptotic events induced by caspase-8 and cytochrome *c* by direct inhibition of distinct caspases. *EMBO J* **17**, 2215–2223.

Egger, D., Wölk, B., Gosert, R., Bianchi, L., Blum, H. E., Moradpour, D. & Bienz, K. (2002). Expression of hepatitis C virus proteins induces distinct membrane alterations including a candidate viral replication complex. *J Virol* **76**, 5974–5984.

Eguchi, Y., Shimizu, S. & Tsujimoto, Y. (1997). Intracellular ATP levels determine cell death fate by apoptosis or necrosis. *Cancer Res* **57**, 1835–1840.

Erdtmann, L., Franck, N., Lerat, H., Seyec, J. L., Gilot, D., Cannie, I., Gripon, P., Hibner, U. & Guguen-Guillouzo, C. (2003). The hepatitis C virus NS2 protein is an inhibitor of CIDE-B-induced apoptosis. *J Biol Chem* **278**, 18256–18264.

Everett, H., Barry, M., Sun, X., Lee, S. F., Frantz, C., Berthiaume, L. G., McFadden, G. & Bleackley, R. C. (2002). The myxoma poxvirus protein, M11L, prevents apoptosis by direct interaction with the mitochondrial permeability transition pore. *J Exp Med* **196**, 1127–1139.

Failla, C., Tomei, L. & De Francesco, R. (1995). An amino-terminal domain of the hepatitis C virus NS3 protease is essential for interaction with NS4A. *J Virol* **69**, 1769–1777.

Fearnhead, H. O., Rodriguez, J., Govek, E.-E., Guo, W., Kobayashi, R., Hannon, G. & Lazebnik, Y. A. (1998). Oncogene-dependent apoptosis is mediated by caspase-9. *Proc Natl Acad Sci U S A* **95**, 13664–13669.

Feng, P., Park, J., Lee, B.-S., Lee, S.-H., Bram, R. J. & Jung, J. U. (2002). Kaposi's sarcoma-associated herpesvirus mitochondrial K7 protein targets a cellular calcium-modulating cyclophilin ligand to modulate intracellular calcium concentration and inhibit apoptosis. *J Virol* **76**, 11491–11504.

Florese, R. H., Nagano-Fujii, M., Iwanaga, Y., Hidajat, R. & Hotta, H. (2002). Inhibition of protein synthesis by the nonstructural proteins NS4A and NS4B of hepatitis C virus. *Virus Res* **90**, 119–131.

Fujita, T., Ishido, S., Muramatsu, S., Itoh, M. & Hotta, H. (1996). Suppression of actinomycin D-induced apoptosis by the NS3 protein of hepatitis C virus. *Biochem Biophys Res Commun* **229**, 825–831.

Gewies, A., Rokhlin, O. W. & Cohen, M. B. (2000). Cytochrome *c* is involved in Fas-mediated apoptosis of prostatic carcinoma cell lines. *Cancer Res* **60**, 2163–2168.

Goldmacher, V. S., Bartle, L. M., Skaletskaya, A. & 10 other authors (1999). A cytomegalovirus-encoded mitochondria-localized inhibitor of apoptosis structurally unrelated to Bcl-2. *Proc Natl Acad Sci U S A* **96**, 12536–12541.

Gosert, R., Egger, D., Lohmann, V., Bartenschlager, R., Blum, H. E., Bienz, K. & Moradpour, D. (2003). Identification of the hepatitis C virus RNA replication complex in Huh-7 cells harboring subgenomic replicons. *J Virol* **77**, 5487–5492.

Gross, A., McDonnell, J. M. & Korsmeyer, S. J. (1999). BCL-2 family members and the mitochondria in apoptosis. *Genes Dev* **13**, 1899–1911.

Hahn, C. S., Cho, Y. G., Kang, B.-S., Lester, I. M. & Hahn, Y. S. (2000). The HCV core protein acts as a positive regulator of Fas-mediated apoptosis in a human lymphoblastoid T cell line. *Virology* **276**, 127–137.

Hayashi, J., Kishihara, Y., Yamaji, K., Furusyo, N., Yamamoto, T., Pae, Y., Etoh, Y., Ikematsu, H. & Kashiwagi, S. (1997). Hepatitis C viral quasispecies and liver damage in patients with chronic hepatitis C virus infection. *Hepatology* **25**, 697–701.

He, Y., Nakao, H., Tan, S.-L., Polyak, S. J., Neddermann, P., Vijaysri, S., Jacobs, B. L. & Katze, M. G. (2002). Subversion of cell signaling pathways by hepatitis C virus nonstructural 5A protein via interaction with Grb2 and P85 phosphatidylinositol 3-kinase. *J Virol* **76**, 9207–9217.

Hidajat, R., Nagano-Fujii, M., Deng, L., Tanaka, M., Takigawa, Y., Kitazawa, S. & Hotta, H. (2005). Hepatitis C virus NS3 protein interacts with ELKS-δ and ELKS-α, members of a novel protein family involved in intracellular transport and secretory pathways. *J Gen Virol* **86**, 2197–2208.

Hiramatsu, N., Hayashi, N., Katayama, K., Mochizuki, K., Kawanishi, Y., Kasahara, A., Fusamoto, H. & Kamada, T. (1994). Immunohistochemical detection of Fas antigen in liver tissue of patients with chronic hepatitis C. *Hepatology* **19**, 1354–1359.

Hsu, E. C., Hsi, B., Hirota-Tsuchihara, M. & 8 other authors (2003). Modified apoptotic molecule (BID) reduces hepatitis C virus infection in mice with chimeric human livers. *Nat Biotechnol* **21**, 519–525.

Ishido, S., Fujita, T. & Hotta, H. (2000). Possible involvement of the NS3 protein of hepatitis C virus in hepatocarcinogenesis: its interaction with the p53 tumor suppressor. In *Hepatocellular Carcinoma: Methods and Protocols*, pp. 37–55. Edited by N. A. Habib. Totowa: Humana Press.

Jacotot, E., Ravagnan, L., Loeffler, M. & 15 other authors (2000). The HIV-1 viral protein R induces apoptosis via a direct effect on the mitochondrial permeability transition pore. *J Exp Med* **191**, 33–45.

Jacotot, E., Ferri, K. F., El Hamel, C. & 17 other authors (2001). Control of mitochondrial membrane permeabilization by adenine nucleotide translocator interacting with HIV-1 viral protein R and Bcl-2. *J Exp Med* **193**, 509–520.

Kato, J., Kato, N., Yoshida, H., Ono-Nita, S. K., Shiratori, Y. & Omata, M. (2002). Hepatitis C virus NS4A and NS4B proteins suppress translation in vivo. *J Med Virol* **66**, 187–199.

Kim, J.-E., Song, W. K., Chung, K. M., Back, S. H. & Jang, S. K. (1999). Subcellular localization of hepatitis C viral proteins in mammalian cells. *Arch Virol* **144**, 329–343.

Kiyosawa, K., Sodeyama, T., Tanaka, E. & 8 other authors (1990). Interrelationship of blood transfusion, non-A, non-B hepatitis and hepatocellular carcinoma: analysis by detection of antibody to hepatitis C virus. *Hepatology* **12**, 671–675.

Kuang, W.-F., Lin, Y.-C., Jean, F., Huang, Y.-W., Tai, C.-L., Chen, D.-S., Chen, P.-J. & Hwang, L.-H. (2004). Hepatitis C virus NS3 RNA helicase activity is modulated by the two domains of NS3 and NS4A. *Biochem Biophys Res Commun* **317**, 211–217.

Lan, K.-H., Sheu, M.-L., Hwang, S.-J. & 8 other authors (2002). HCV NS5A interacts with p53 and inhibits p53-mediated apoptosis. *Oncogene* **21**, 4801–4811.

Leprat, P., Ratinaud, M. H., Maftah, A., Petit, J. M. & Julien, R. (1990). Use of nonyl acridine orange and rhodamine 123 to follow biosynthesis and functional assembly of mitochondrial membrane during L1210 cell cycle. *Exp Cell Res* **186**, 130–137.

Li, L., Lorenzo, P. S., Bogi, K., Blumberg, P. M. & Yuspa, S. H. (1999). Protein kinase Cδ targets mitochondria, alters mitochondrial membrane potential, and induces apoptosis in normal and neoplastic keratinocytes when overexpressed by an adenoviral vector. *Mol Cell Biol* **19**, 8547–8558.

Li, X.-D., Sun, L., Seth, R. B., Pineda, G. & Chen, Z. J. (2005). Hepatitis C virus protease NS3/4A cleaves mitochondrial antiviral signaling protein off the mitochondria to evade innate immunity. *Proc Natl Acad Sci U S A* **102**, 17717–17722.

Lin, C.-F., Chen, C.-L., Chang, W.-T., Jan, M.-S., Hsu, L.-J., Wu, R.-H., Tang, M.-J., Chang, W.-C. & Lin, Y.-S. (2004). Sequential caspase-2 and caspase-8 activation upstream of mitochondria during ceramide- and etoposide-induced apoptosis. *J Biol Chem* **279**, 40755–40761.

Liu, X., Kim, C. N., Yang, J., Jemmerson, R. & Wang, X. (1996). Induction of apoptotic program in cell-free extracts: requirement for dATP and cytochrome c. *Cell* **86**, 147–157.

Lohmann, V., Körner, F., Dobierzewska, A. & Bartenschlager, R. (2001). Mutations in hepatitis C virus RNAs conferring cell culture adaptation. *J Virol* **75**, 1437–1449.

Moorman, J. P., Prayther, D., McVay, D., Hahn, Y. S. & Hahn, C. S. (2003). The C-terminal region of hepatitis C core protein is required for Fas-ligand independent apoptosis in Jurkat cells by facilitating Fas oligomerization. *Virology* **312**, 320–329.

Mottola, G., Cardinali, G., Ceccacci, A., Trozzi, C., Bartholomew, L., Torrisi, M. R., Pedrazzini, E., Bonatti, S. & Migliaccio, G. (2002). Hepatitis C virus nonstructural proteins are localized in a modified endoplasmic reticulum of cells expressing viral subgenomic replicons. *Virology* **293**, 31–43.

Muramatsu, S., Ishido, S., Fujita, T., Itoh, M. & Hotta, H. (1997). Nuclear localization of the NS3 protein of hepatitis C virus and factors affecting the localization. *J Virol* **71**, 4954–4961.

Muzio, M., Chinnaiyan, A. M., Kischkel, F. C. & 11 other authors (1996). FLICE, a novel FADD-homologous ICE/CED-3-like protease, is recruited to the CD95 (Fas/APO-1) death-inducing signaling complex. *Cell* **85**, 817–827.

Pang, P. S., Jankowsky, E., Planet, P. J. & Pyle, A. M. (2002). The hepatitis C viral NS3 protein is a processive DNA helicase with cofactor enhanced RNA unwinding. *EMBO J* **21**, 1168–1176.

Rahmani, Z., Huh, K.-W., Lasher, R. & Siddiqui, A. (2000). Hepatitis B virus X protein colocalizes to mitochondria with a human voltage-dependent anion channel, HVDAC3, and alters its transmembrane potential. *J Virol* **74**, 2840–2846.

Reed, K. E. & Rice, C. M. (2000). Overview of hepatitis C virus genome structure, polyprotein processing, and protein properties. *Curr Top Microbiol Immunol* **242**, 55–84.

Ruggieri, A., Harada, T., Matsuura, Y. & Miyamura, T. (1997). Sensitization to Fas-mediated apoptosis by hepatitis C virus core protein. *Virology* **229**, 68–76.

Ruggieri, A., Murdolo, M. & Rapicetta, M. (2003). Induction of FAS ligand expression in a human hepatoblastoma cell line by HCV core protein. *Virus Res* **97**, 103–110.

Sacco, R., Tsutsumi, T., Suzuki, R. & 8 other authors (2003). Antiapoptotic regulation by hepatitis C virus core protein through up-regulation of inhibitor of caspase-activated DNase. *Virology* **317**, 24–35.

Satoh, S., Tanji, Y., Hijikata, M., Kimura, K. & Shimotohno, K. (1995). The N-terminal region of hepatitis C virus nonstructural protein 3 (NS3) is essential for stable complex formation with NS4A. *J Virol* **69**, 4255–4260.

Schwer, B., Ren, S., Pietschmann, T., Kartenbeck, J., Kaehlcke, K., Bartenschlager, R., Yen, T. S. B. & Ott, M. (2004). Targeting of hepatitis C virus core protein to mitochondria through a novel C-terminal localization motif. *J Virol* **78**, 7958–7968.

Shu, H.-B., Halpin, D. R. & Goeddel, D. V. (1997). Casper is a FADD- and caspase-related inducer of apoptosis. *Immunity* **6**, 751–763.

Siavoshian, S., Abraham, J. D., Thumann, C., Kieny, M. P. & Schuster, C. (2005). Hepatitis C virus core, NS3, NS5A, NS5B proteins induce apoptosis in mature dendritic cells. *J Med Virol* **75**, 402–411.

Skulachev, V. P. (1998). Cytochrome *c* in the apoptotic and antioxidant cascades. *FEBS Lett* **423**, 275–280.

Soguero, C., Joo, M., Chianese-Bullock, K. A., Nguyen, D. T., Tung, K. & Hahn, Y. S. (2002). Hepatitis C virus core protein leads to immune suppression and liver damage in a transgenic murine model. *J Virol* **76**, 9345–9354.

Song, J., Fujii, M., Wang, F., Itoh, M. & Hotta, H. (1999). The NS5A protein of hepatitis C virus partially inhibits the antiviral activity of interferon. *J Gen Virol* **80**, 879–886.

Sung, V. M.-H., Shimodaira, S., Doughty, A. L., Picchio, G. R., Can, H., Yen, T. S. B., Lindsay, K. L., Levine, A. M. & Lai, M. M. C. (2003). Establishment of B-cell lymphoma cell lines persistently infected with hepatitis C virus in vivo and in vitro: the apoptotic effects of virus infection. *J Virol* **77**, 2134–2146.

Taguchi, T., Nagano-Fujii, M., Akutsu, M., Kadoya, H., Ohgimoto, S., Ishido, S. & Hotta, H. (2004). Hepatitis C virus NS5A protein interacts with 2′,5′-oligoadenylate synthetase and inhibits antiviral activity of IFN in an IFN sensitivity-determining region-independent manner. *J Gen Virol* **85**, 959–969.

Takigawa, Y., Nagano-Fujii, M., Deng, L., Hidajat, R., Tanaka, M., Mizuta, H. & Hotta, H. (2004). Suppression of hepatitis C virus replicon by RNA interference directed against the NS3 and NS5B regions of the viral genome. *Microbiol Immunol* **48**, 591–598.

Tong, M. J., El-Farra, N. S., Reikes, A. R. & Co, R. L. (1995). Clinical outcomes after transfusion-associated hepatitis C. *N Engl J Med* **332**, 1463–1466.

Wang, F., Yoshida, I., Takamatsu, M., Ishido, S., Fujita, T., Oka, K. & Hotta, H. (2000). Complex formation between hepatitis C virus core protein and p21Waf1/Cip1/Sdi1. *Biochem Biophys Res Commun* **273**, 479–484.

Wang, H.-W., Sharp, T. V., Koumi, A., Koentges, G. & Boshoff, C. (2002). Characterization of an anti-apoptotic glycoprotein encoded by Kaposi's sarcoma-associated herpesvirus which resembles a spliced variant of human survivin. *EMBO J* **21**, 2602–2615.

Wölk, B., Sansonno, D., Kräusslich, H.-G., Dammacco, F., Rice, C. M., Blum, H. E. & Moradpour, D. (2000). Subcellular localization, stability, and *trans*-cleavage competence of the hepatitis C virus NS3-NS4A complex expressed in tetracycline-regulated cell lines. *J Virol* **74**, 2293–2304.

Zhu, N., Ware, C. F. & Lai, M. M. (2001). Hepatitis C virus core protein enhances FADD-mediated apoptosis and suppresses TRADD signaling of tumor necrosis factor receptor. *Virology* **283**, 178–187.

Journal of General Virology (2006), 87, 1703–1713 DOI 10.1099/vir.0.81735-0

NS3 protein of *Hepatitis C virus* associates with the tumour suppressor p53 and inhibits its function in an NS3 sequence-dependent manner

Lin Deng,[1] Motoko Nagano-Fujii,[1] Motofumi Tanaka,[1,2] Yuki Nomura-Takigawa,[1] Masanori Ikeda,[3] Nobuyuki Kato,[3] Kiyonao Sada[1] and Hak Hotta[1]

Correspondence
Hak Hotta
hotta@kobe-u.ac.jp

[1,2]Divisions of Microbiology[1] and Gastroenterological Surgery[2], Kobe University Graduate School of Medicine, Kobe 650-0017, Japan

[3]Department of Molecular Biology, Okayama University Graduate School of Medicine and Dentistry, Okayama 700-8558, Japan

The N-terminal 198 residues of NS3 (NS3-N) of *Hepatitis C virus* (HCV) subtype 1b obtained from 29 patients, as well as full-length NS3 (NS3-Full), were analysed for their subcellular localization, interaction with the tumour suppressor p53 and serine protease activity in the presence and absence of the viral cofactor NS4A. Based on the subcellular-localization patterns in the absence of NS4A, NS3-N sequences were classified into three groups, with each group exhibiting either dot-like, diffuse or a mixed type of localization. Chimeric NS3-Full sequences, each consisting of an individual NS3-N and a shared C-terminal sequence, showed the same localization patterns as those of the respective NS3-N. Site-directed mutagenesis experiments revealed that a single or a few amino acid substitutions at a particular position(s) of NS3-N altered the localization pattern. Interestingly, NS3 of the dot-like type, either NS3-N or NS3-Full, interacted with p53 more strongly than that of the diffuse type, in both the presence and the absence of NS4A. Moreover, NS3-N of the dot-like type suppressed *trans*-activating activity of p53 more strongly than that of the diffuse type. Serine protease activity did not differ significantly between the two types of NS3. In HCV RNA replicon-harbouring cells, physical interaction between NS3 and p53 was observed consistently and p53-mediated transcriptional activation was suppressed significantly compared with HCV RNA-negative control cells. Our results collectively suggest the possibility that NS3 plays an important role in the hepatocarcinogenesis of HCV by interacting differentially with p53 in an NS3 sequence-dependent manner.

Received 5 December 2005
Accepted 30 January 2006

INTRODUCTION

Chronic, persistent infection with *Hepatitis C virus* (HCV) often leads to liver cirrhosis and hepatocellular carcinoma (HCC) (Saito *et al.*, 1990). However, the exact mechanisms of HCV-associated pathogenesis and carcinogenesis are largely unknown.

HCV possesses a single-stranded, positive-sense RNA genome of 9·6 kb, which encodes a polyprotein of approximately 3000 aa. The polyprotein is processed into at least 10 structural and non-structural (NS) viral proteins by cellular and viral proteases (Reed & Rice, 2000). One of the viral proteases, the NS3 serine protease, has become a research focus, as it is indispensable for virus replication and, therefore, would be a good target for antiviral drugs. The serine protease is encoded in the N-terminal portion of NS3 and is responsible for cleavage at the NS3/4A, NS4A/4B, NS4B/5A and NS5A/5B junctions. NS4A, a cofactor for NS3, stabilizes it to augment its serine protease activity, being virtually essential for complete cleavage of the HCV polyprotein (Reed & Rice, 2000). The C-terminal portion of NS3 possesses the NTPase/helicase activity (Kim *et al.*, 1995), which is essential for viral RNA replication.

In addition to its key role in the life cycle of HCV, possible involvement of NS3 in viral persistence and hepatocarcinogenesis has been studied. For example, NS3 was reported to transform NIH3T3 (Sakamuro *et al.*, 1995) and rat fibroblast (Zemel *et al.*, 2001) cells. We also demonstrated that NIH3T3 cells constitutively expressing C-terminally truncated NS3 (aa 1–433) were more resistant to actinomycin D-induced apoptosis than control cells (Fujita *et al.*, 1996). It was also reported that NS3 could block transforming growth factor-β/Smad3-mediated apoptosis (Cheng *et al.*,

Supplementary figures showing subcellular-localization patterns and a sequence alignment are available in JGV Online.